International Immunopharmacology 174 (2026) 116380

Contents lists available at ScienceDirect

International Immunopharmacology

journal homepage: www.elsevier.com/locate/intimp

VEGFR-1 blockade with the monoclonal antibody D16F7 counteracts VEGF-A-induced tolerogenic and immune regulatory phenotypes without impairing T-cell activation

Ornella Franzese [a,*], Belinda Palermo [b], Pedro Miguel Lacal [c], Grazia Graziani [a,*]

[a] Department of Systems Medicine, University of Rome Tor Vergata, Via Montpellier 1, 00133 Rome, Italy
[b] Tumor Immunology and Immunotherapy Unit, IRCCS-Regina Elena National Cancer Institute, Via Elio Chianesi 53, 00144, Rome, Italy
[c] Laboratory of Molecular Oncology, IDI-IRCCS, Via Monti di Creta 104, 00167 Rome, Italy

ARTICLE INFO

Editor Name: Dr. Raheleh Roudi

Keywords:
VEGF-A
D16F7
VEGFR-1
T cells
Dendritic cells
Immune checkpoints

ABSTRACT

Objective: VEGF-A exerts complex immunomodulatory effects that foster an immunosuppressive tumour microenvironment, including impaired dendritic cell (DC) maturation, expansion of regulatory T cells (Tregs), and induction of T-cell exhaustion, while transiently enhancing effector T-cell responses. This dual activity underscores the need to clarify the immunosuppressive versus immunostimulatory consequences of VEGF-A receptor activation to optimise selective inhibition. This proof-of-concept study evaluated whether selective VEGFR-1 blockade can counteract VEGF-A-driven immunosuppression in human immune cells using the monoclonal antibody (mAb) D16F7, which inhibits membrane-bound VEGFR-1 while preserving the decoy and anti-angiogenic activity of its soluble form.

Methods: The impact of VEGFR-1 blockade by D16F7 mAb on VEGF-A-mediated immune modulation was assessed by multiparametric flow cytometry using primary immune cells from healthy donors. Human DCs were generated from $CD14^{+}$ monocytes and cultured with VEGF-A; tolerogenic and pro-exhaustion activity was evaluated via maturation markers (CD80, CD83, HLA-DR) and PD-1 expression on DC-stimulated T cells after 14 days. Short-term effects on effector T cells, stratified by PD-1 and CD28 expression, were analysed by intracellular cytokine staining at 5–6 and 18 h. Purified Tregs, isolated via a two-step magnetic separation, were cultured for 1 week to assess the acquisition of an immunosuppressive phenotype by measuring the expression of checkpoint markers (PD-1, ICOS, TIM-3).

Results: D16F7 reversed VEGF-A-induced DC maturation defects, reduced DC-mediated T-cell tolerance, and attenuated the emergence of a highly immunosuppressive Treg phenotype, while largely preserving short-term effector T-cell function.

Conclusions: Despite the limitations of an in vitro PBMC-based system, selective VEGFR-1 blockade by D16F7 mAb alleviates VEGF-A-driven immune tolerance while preserving T-cell activation, supporting its translational potential as a complementary immunomodulatory approach.

1. Introduction

Vascular Endothelial Growth Factor-A (VEGF-A) is a key regulator of angiogenesis, promoting endothelial cell proliferation, migration, survival, and vascular permeability [1]. These effects are mediated by two high-affinity tyrosine kinase receptors, VEGFR-1 (Flt-1) and VEGFR-2 (KDR/Flk-1), which exhibit distinct yet complementary roles in angiogenesis, tumour invasiveness and immune regulation [2]. Beyond its canonical vascular functions, VEGF-A exerts profound immunoregulatory effects through both direct and indirect mechanisms [3]. Within the tumour microenvironment (TME), VEGF-A-driven vascular abnormalities impair T-cell infiltration [4], downregulate adhesion molecules, and create physical barriers that limit T-cell migration and adhesion, collectively fostering immune evasion and sustaining irregular angiogenesis [5,6].

VEGF-A further promotes an immunosuppressive TME by enhancing the accumulation of myeloid-derived suppressor cells (MDSCs) [7] and interfering with dendritic cell (DC) differentiation [8]. This results in

* Corresponding authors.
E-mail addresses: franzese@uniroma2.it (O. Franzese), graziani@uniroma2.it (G. Graziani).

https://doi.org/10.1016/j.intimp.2026.116380
Received 5 December 2025; Received in revised form 5 February 2026; Accepted 9 February 2026
Available online 17 February 2026

defective antigen (Ag) presentation and tolerance induction. Elevated VEGF-A levels in cancer patients correlate with immature DCs [9], which in turn facilitate regulatory T-cell (Treg) generation and tolerogenic T-cell responses [10,11]. VEGF-A also contributes to a hypoxic and acidic TME, reinforcing the recruitment and activity of Tregs, MDSCs, and M2 tumour-associated macrophages (TAMs) [12].

Tregs are central regulators of immune homeostasis, suppressing effector T-cell responses and promoting tolerance in both transplantation [13] and cancer, where they support immune evasion and resistance to immunotherapy [14]. In tumours, VEGF-A contributes to the expansion of Tregs via VEGFR-2, either by enhancing their proliferation or by converting conventional $CD4^+$ T cells into regulatory phenotypes [3]. Accordingly, elevated Treg frequency is consistently associated with poor prognosis [15–17]. While VEGFR-2 plays a major role in maintaining Treg suppressive function [18], a distinct $CD4^+$ Treg subset characterised by high levels of VEGFR-1 has also been identified, exhibiting strong immunosuppressive activity by inhibiting conventional T-cell proliferation and dampening inflammatory responses [19].

The effects of VEGF-A on effector T cells are context- and time-dependent. Sustained VEGF-A exposure can suppress the proliferation of T cells isolated from ovarian cancer ascites via VEGFR-2 signalling [20]. In microsatellite-stable colorectal cancer, VEGF-A drives T-cell exhaustion through TOX upregulation, leading to resistance to PD-1 blockade [21] and increased expression of inhibitory checkpoints, including PD-1, CTLA-4, TIM-3, and LAG-3 [22]. Conversely, under certain conditions, VEGF-A can enhance T-cell activation, promoting IFN-γ release from $CD45RO^+$ memory $CD4^+$ T cells via ERK/AKT signalling [23] or augmenting $CD4^+$ cytotoxic T-cell function through AKT/mTOR pathways [24]. These findings underscore the multifaceted, context-dependent immunomodulatory role of VEGF-A.

Importantly, unlike VEGFR-2, VEGFR-1 is dispensable for physiological angiogenesis in adults but is crucial for pathological angiogenesis, including tumour-associated neo vessel formation [25]. VEGFR-1 also regulates the mobilisation of myeloid progenitors and recruitment of M2 TAMs [26], highlighting its dual role in angiogenesis and immune regulation. Activated human $CD4^+$ and $CD8^+$ T cells express VEGFR-1, suggesting a direct role in VEGF-A-mediated modulation of lymphocyte function [27]. These findings collectively identify VEGFR-1 as a promising therapeutic target to counteract VEGF-A-driven immunosuppression and reshape the tumour immune landscape.

Based on this evidence, we investigated the immunomodulatory effects of the anti-VEGFR-1 monoclonal antibody (mAb) D16F7 that selectively inhibits VEGFR-1 activation by a non-competitive mechanism (i.e., without hampering ligand binding). Its unique mechanism of action allows to preserve the decoy function of the soluble VEGFR-1 (sVEGFR-1) forms that sequester VEGF-A in the extra-cellular matrix, contributing to restrain angiogenesis and tumour invasiveness [28–30].

The selective blockade of VEGFR-1 with the D16F7 mAb can provide a useful strategy to dissect VEGFR-1-dependent outcomes in DCs and T cells. Herein, we examined how VEGFR-1 inhibition shapes VEGF-A-driven immune modulation, focusing on three key processes: the induction of immature or tolerogenic DCs, the acquisition of suppressive phenotypes by Tregs, and the functional responses of conventional T-cell subsets characterised by PD-1 and CD28 expression. These two molecules are central regulators of T-cell activation and exhaustion and serve as important biomarkers of clinical responses to immune checkpoint inhibitors (ICIs) [31–33]. Of relevance, PD-1 blockade has been shown to preferentially reinvigorate a $CD28^+$ progenitor-like subset of exhausted $CD8^+$ T cells. By contrast, $PD\text{-}1^+CD28^-$ $CD8^+$ T cells represent a terminally exhausted subset that lacks the CD28-dependent costimulatory machinery required for the proliferative burst induced by PD-1 inhibition [34] and therefore responds poorly to anti-PD-1 therapies.

Indeed, the D16F7 mAb has been shown to recognise not only the human VEGFR-1 but also the murine receptor [28] allowing to demonstrate that it exerts antitumor activity in a syngeneic melanoma model, where it reduces tumour growth and reshapes the TME by limiting M2 macrophage, $PD\text{-}1^+$ T cell, and Treg infiltration [35]. Building on these in vivo observations, the present study provides an immune-cell-focused proof-of-concept analysis in a human context, complementing prior murine work and highlighting the immunomodulatory potential of VEGFR-1 inhibition.

Our results indicate that VEGFR-1 inhibition with the D16F7 mAb counteracts VEGF-A-driven impairment of DC maturation and tolerogenic skewing, preserves T-cell effector functionality, and reduces the acquisition of an immunosuppressive Treg phenotype. These findings suggest that selective VEGFR-1 blockade may not only hamper pathological angiogenesis and tumour invasiveness [28–30] but also serve as a promising immunomodulatory approach.

2. Material and methods

2.1. Peripheral blood mononuclear cell (PBMC) isolation and culture

PBMCs were isolated from buffy coat samples obtained from healthy donors by Ficoll-Hypaque (Pharmacia, Uppsala, Sweden) by density gradient centrifugation. Cells were resuspended in RPMI 1640 medium (Life Technologies, Carlsbad, CA, USA) supplemented with 10% foetal calf serum (FCS; Life Technologies), 2 mM L-glutamine (Flow Laboratories, Irvine, UK), and 100 IU/mL penicillin-streptomycin (Life Technologies). Cultures were maintained at 37°C in a humidified 5% CO_2 incubator.

2.2. Flow cytometry and intracellular cytokine staining

Surface marker staining was performed at 4°C for 30 min using fluorochrome-conjugated mAbs: BV605 anti-human CD8 (BD Biosciences, Franklin Lakes, NJ, USA; cat. no. 564115), BV650 anti-human PD-1 (BD; 564104), APC-R700 anti-human CD28 (BD; 565181), BB700 anti-human CD4 (BD; 566392), BV786 anti-human ICOS (BD; 567922), BB515 anti-human TIM-3/CD366 (BD; 565568), BV421 anti-human CD80 (BD; 564160), PE anti-human HLA-DR (BD; 555812), FITC anti-human CD83 (BD; 556910), BV786 anti-human VEGFR-2/CD309 (BD; 759690), and PE anti-human VEGFR-1/Flt-1 (R&D Systems, Bio-Techne, Minneapolis, MN, USA; FAB321P), together with matched isotype controls (BD).

Intracellular cytokine staining was carried out using the BD IntraSure kit (BD; 641778), following the manufacturer's instructions. The following mAbs were used: APC anti-human tumour necrosis factor α (TNF-α) (BD; 554514), BV480 anti-human interferon γ (IFN-γ) (BD; 566176), and BV421 anti-human granzyme B (GrzB) (BD; 563389).

For functional assays, 2–3 × 10^5 cells were stimulated with plate-bound anti-CD3 mAb (OKT3, functional grade; eBioscience, San Diego, CA, USA; cat. no. 16-0037-81) and recombinant human (rh) interleukin (IL)-2 (5 ng/mL; R&D Systems, Minneapolis, MN, USA) with or without 50 ng/mL $rhVEGF\text{-}A_{165}$ (ImmunoTools; cat. no. 11343665), with or without the anti-VEGFR-1 mAb D16F7 [27] (5 μg/mL) or the anti-VEGFR-2 mAb ramucirumab (Thermo Fisher Scientific, Waltham, MA, USA; cat. no. MA5-58411) (10 μg/mL) for 5–6 hours (h), 18 h or 24 h in the presence of the protein transport inhibitors GolgiStop (BD Biosciences, Franklin Lakes, NJ, USA; cat. no. 554724) and GolgiPlug (BD; cat. no. 555029), when required. After stimulation, cells were stained with appropriate combinations of labelled mAbs for surface and intracellular markers as indicated.

Flow cytometric acquisition was performed using a BD FACSCelesta flow cytometer (BD Biosciences), and data were analysed with BD FACSDiva software. Results were expressed as the percentage of marker-positive cells or as mean fluorescence intensity (MFI), calculated as the product of the percentage of positive cells and their mean fluorescence value (MFV). When indicated, MFI and percentage values were normalized as fold changes relative to untreated controls (set to 1).

2.3. In vitro generation, phenotypical and functional analysis of human DCs

Monocytes were purified from PBMCs using anti-human CD14 magnetic microbeads (Miltenyi Biotec, Bergisch Gladbach, Germany; cat. no. 130-097-052) according to the manufacturer's instructions. Briefly, PBMCs were incubated with anti-CD14 microbeads for 15 min at 4 °C, washed, and passed through a magnetic separation column to isolate $CD14^+$ monocytes. Purified monocytes were counted and resuspended in RPMI 1640 medium supplemented with 10% heat-inactivated foetal bovine serum and antibiotics.

Monocytes were seeded at 0.5–1 $\times$ 10^6 cells/mL and cultured for six days in the presence of 500 IU/mL rh granulocyte-macrophage colony-stimulating factor (GM-CSF; ImmunoTools, Friesoythe, Germany; cat. no. 12343125) and 500 IU/mL rh IL-4 (ImmunoTools; cat. no. 11340045) to induce differentiation into immature DCs. On day 3, half of the culture medium was replaced with fresh medium containing the same cytokine concentrations. Cultures were performed in the absence or presence of rhVEGF-A_{165} (50 ng/mL), with or without the anti-VEGFR-1 mAb D16F7 [28] (5 μg/mL) or the anti-VEGFR-2 mAb ramucirumab (10 μg/mL). On day 6, DC maturation was induced by adding rhTNF-α (100 ng/mL; ImmunoTools; cat. no. 11343015) or lipopolysaccharide (LPS, 100 ng/mL; Sigma-Aldrich–Merck, Saint Louis, MO, USA; cat. no. L439). Cells were incubated for additional 24-48 h before harvesting mature DCs. VEGF-A (50 ng/mL) and the anti-VEGFR-1 mAb D16F7 (5 μg/mL) and, in selected experiments, the anti-VEGFR-2 mAb ramucirumab (10 μg/mL) were added at culture initiation, on day 3 during medium change, and again at the maturation stage. DCs were visualized and photographed using a Nikon Eclipse TS100 microscope in conjunction with a Nikon DS-Fi1 high resolution camera (Melville, NY). Mature DCs were analysed morphologically and by flow cytometry following staining with anti-human CD80, CD83, and HLA-DR mAbs (all from BD Biosciences).

2.4. Co-cultures of tolerogenic DCs with autologous and allogeneic T cells

To evaluate the tolerogenic activity of VEGF-A and the potential antagonistic effect of the anti-VEGFR-1 mAb D16F7, mature $CD14^+$-derived DCs were loaded with a pool of viral peptides (PepTivator CEF MHC Class I Plus-hu; Miltenyi Biotec, cat. no. 130-042-401), according to the manufacturer's instructions, and co-cultured with autologous $CD14^-$ cells in complete RPMI 1640 medium supplemented with 5% human serum (Sigma-Aldrich–Merck, Saint Louis, MO, USA; cat. no. P2918) plus 5 ng/mL rhIL-2, at a 10:1 T cell/DC ratio in 96-well flat-bottom plates (200 μL per well).

For allogeneic mixed lymphocyte reaction (MLR) assays, $CD14^-$ T cells were isolated from PBMCs of unrelated healthy donors and co-cultured with allogeneic DCs at a 10:1 T cell/DC ratio in 96-well flat-bottom plates (200 μL per well). Co-cultures were maintained for 14 days at 37°C in a humidified 5% CO_2 incubator, with fresh medium supplemented with rhIL-2 (5 ng/mL) added every 3 days. At day 14, expression of the exhaustion marker PD-1 on $CD8^+$ and $CD4^+$ T-cell subsets, and the frequency of T-cell subsets characterized by PD-1 and/or CD28 expression was assessed by flow cytometry by using standard staining protocols.

2.5. Isolation and culture of Tregs

Highly purified $CD4^+$ Tregs were isolated from PBMCs of healthy donors using the $CD4^+CD25^+CD127^-$dim Regulatory T-cell Isolation Kit (Miltenyi Biotec, cat. no. 130-094-775), by a two-step magnetic separation following the manufacturer's instructions. Purified Tregs were stimulated with plate-bound anti-human CD3 mAb, soluble anti-human CD28 mAb (clone CD28.6; eBioscience, San Diego, CA, USA; cat. no. 16-0288-81), and rhIL-2 (5 ng/mL).

Cells were cultured for 7 days in the presence or absence of rhVEGF-A (50 ng/mL), either alone or combined with the anti-VEGFR-1 mAb D16F7 (5 μg/mL) or the anti-VEGFR-2 mAb ramucirumab (10 μg/mL). Fresh medium containing rhIL-2 and the respective treatments (VEGF-A, D16F7 mAb, or ramucirumab) was replenished every 3 days. After 7 days, surface expression of PD-1, ICOS, and TIM-3 on Tregs was analysed by flow cytometry using standard staining procedures, as above described.

2.6. Statistical analysis

Statistical analysis was performed using GraphPad Prism version 9.3.1 (GraphPad Software, San Diego, CA, USA). Two-tailed paired *t*-tests were applied for pairwise comparisons. For each treatment condition, comparisons included VEGF-A versus control, and VEGF-A combined with anti-VEGFR-1 (D16F7) or anti-VEGFR-2 (ramucirumab) versus VEGF-A alone. *P* values <0.05 were considered statistically significant, while P values >0.05 and ≤ 0.1 were interpreted as indicating a trend toward significance. Data presented in column graphs are expressed as mean $\pm$ standard deviation (SD). Box plots indicate minimum and maximum values (whiskers) and display the median (horizontal line within the box).

3. Results

3.1. Subset-specific expression of VEGFR-1 and VEGFR-2 suggests distinct roles in $CD8^+$ and $CD4^+$ T-cell activation and exhaustion

CD28, a co-stimulatory receptor essential for delivering the "second signal" during T-cell activation, has recently emerged as a critical determinant of responsiveness to ICIs, particularly anti-PD-1 mAbs [31–34]. Mechanistic studies by Hui et al. demonstrated that PD-1 primarily inhibits T-cell activity by blocking CD28 signalling, and that restoration of this pathway is essential for the anti-PD-1-mediated reinvigoration of exhausted $CD8^+$ T cells [31].

Because VEGF-A functions not only as an immunosuppressive factor but also as a broader immunomodulator within the TME [9], blockade of its signalling can produce heterogeneous immunologic effects. Accordingly, the expression patterns of VEGF-A receptors may help identify T-cell subsets whose functionality is most likely to be modulated by selective activation of VEGFR-1 or VEGFR-2.

To investigate the potential impact of VEGF-A on phenotypically and functionally distinct T-cell subsets, we analysed baseline VEGFR-1 and VEGFR-2 expression in $CD8^+$ and $CD4^+$ T cells from healthy donor PBMCs, stratified by PD-1 and CD28 expression. We specifically compared VEGFR-1 and VEGFR-2 levels between $PD\text{-}1^+$ subsets and their $PD\text{-}1^-$ counterparts ($PD\text{-}1^-CD28^-$ and $PD\text{-}1^-CD28^+$) to determine whether receptor expression correlates with PD-1-associated exhaustion, activation, or differentiation status.

In $CD8^+$ T cells, VEGFR-1 expression was higher in $PD\text{-}1^+$ subsets, with a strong trend observed between $PD\text{-}1^+CD28^-$ and $PD\text{-}1^-CD28^-$ cells ($p=0.06$), and reaching statistical significance when comparing $PD\text{-}1^+CD28^+$ versus the $PD\text{-}1^-CD28^-$ subset ($p=0.02$) (Fig. 1A, upper panel), as measured by MFI. Among $CD4^+$ T-cell subsets, VEGFR-1 differences were not statistically significant (Fig. 1A, lower panel).

Overall, this expression pattern suggests that VEGF-A, via VEGFR-1 engagement, primarily modulates $CD8^+$ T-cell function within $PD\text{-}1^+$ subsets, which already exhibit a checkpoint-associated dysfunctional phenotype. VEGFR-2 expression was consistently higher than VEGFR-1 across all T-cell subsets (Supplementary Fig. 1) and showed only limited variation among the different populations (Fig. 1B).

To investigate how T-cell activation influences VEGFR expression, PBMCs from healthy donors were stimulated with plate-bound anti-CD3 mAb in the presence of rhIL-2 for 24 h. Because PD-1 is rapidly induced upon T-cell activation [36,37] and CD28 expression is also dynamically regulated following stimulation [38], PD-1/CD28-based subset discrimination was not used post-stimulation. Instead, expression of

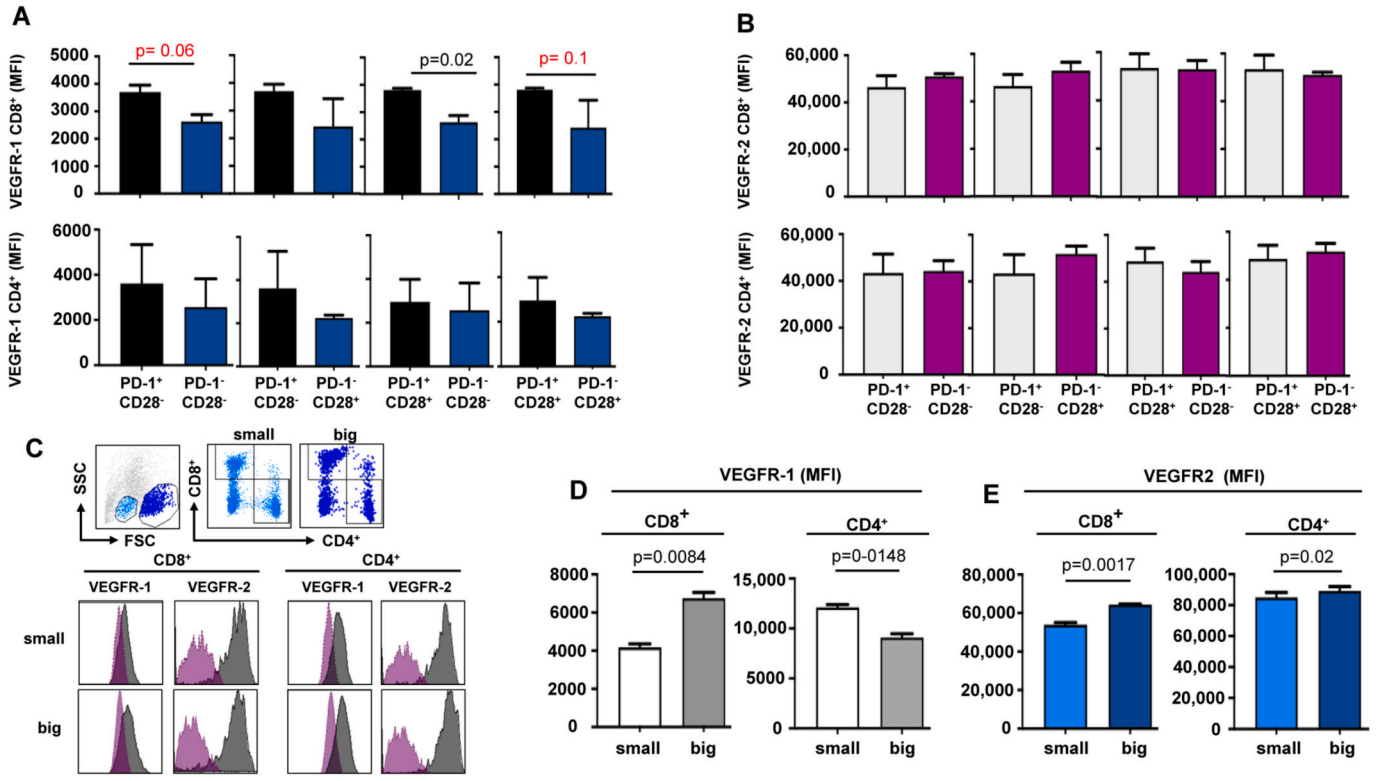

Fig. 1. VEGFR-1 and VEGFR-2 expression in total CD8$^+$ and CD4$^+$ T cells and PD-1/CD28-defined subsets at baseline and after activation. PBMCs from healthy donors were analysed at baseline (A,B) or after 24 h stimulation with plate-bound anti-CD3 mAb and rhIL-2 (C–E) by flow-cytometry. (A) Comparison of VEGFR-1 and VEGFR-2 between PD-1$^+$ and PD-1$^-$ subsets shows significantly higher VEGFR-1 in CD8$^+$PD-1$^+$ T cells. (B) In CD4$^+$ T cells, VEGFR-1 and VEGFR-2 expression differences between PD-1$^+$ and PD-1$^-$ subsets are not significant. (C) Gating strategy for large and small lymphocyte populations (FSC/SSC) after 24 h stimulation, with representative histograms of VEGFR-1 and VEGFR-2 expression in small (unstimulated) versus large (stimulated) CD8$^+$ and CD4$^+$ T cells. (D) VEGFR-1 is significantly higher in large CD8$^+$ T cells and small non-stimulated CD4$^+$ T cells. (E) VEGFR-2 shows a modest but significant increase in large CD8$^+$ T cells. Data are shown as mean ± SD from $n = 3$ independent donors. Two-tailed paired *t*-tests were used for pairwise comparisons; $p \leq 0.05$ was considered significant.

VEGFR-1 and VEGFR-2 was analysed in total CD8$^+$ and CD4$^+$ T-cell populations, enabling an unbiased assessment of receptor modulation under activation conditions without confounding effects from phenotypic remodelling. Forward scatter (FSC) and side scatter (SSC) parameters were used to distinguish small, resting (unstimulated) lymphocytes from larger, activated (stimulated) cells, based on differences in size and internal complexity [39] (Fig. 1C).

When comparing unstimulated (small cell size) and activated (large cell size) T-cell populations, VEGFR-1 expression was significantly increased in big/activated CD8$^+$ T cells (p=0.0084), whereas an opposite pattern was observed in CD4$^+$ T cells, where VEGFR-1 levels were reduced upon activation (p=0.0148) (Fig. 1D). This opposite trend suggests distinct regulatory mechanisms between cytotoxic and helper compartments.

In CD8$^+$ T cells, VEGFR-2 was also modestly but significantly upregulated in the activated population (p=0.0017) (Fig. 1E).

3.2. *The anti VEGF-R1 mAb D16F7 counteracts VEGF-A-mediated induction of tolerogenic DCs*

VEGF-A can impair DC maturation by engaging VEGFR-1 [40]. Indeed, VEGF-A-conditioned DCs exhibit reduced capacity to mature and present Ags, ultimately impairing the generation of effective effector T cells [41]. Based on this evidence, we aimed to determine whether VEGFR-1 blockade with the D16F7 mAb could counteract the tolerogenic effects of VEGF-A on DC differentiation and maturation.

DCs were generated from purified CD14$^+$ monocytes isolated from PBMCs of healthy donors, as described in the Materials and Methods section. Phenotypic maturation was induced using TNF-α (100 ng/mL) or LPS (100 ng/mL), two well-characterised stimuli of DC differentiation. TNF-α promotes the transition of immature monocyte-derived DCs into a mature Ag-presenting phenotype [42], whereas LPS activates maturation through TLR4 signalling, enhances co-stimulatory molecule expression and cytokine release [43].

Maturation was assessed by evaluating CD80 and CD83, key indicators of DC survival and T-cell priming activity [44–47], and HLA-DR, a major histocompatibility complex class II molecule, essential for Ag presentation and full T-cell stimulatory capacity [47]. Consistent with Lu et al. [48], control DCs formed large clusters of non-adherent cells with short dendrites, whereas VEGF-A-conditioned DCs became adherent with elongated, spindle-shaped dendrites, displaying an endothelial-like morphology (Fig. 2A). VEGFR-1 inhibition partially reversed this phenotype, yielding a mixed population of rounded, non-adherent cells and fewer spindle-shaped dendritic forms (Fig. 2A).

Under these experimental conditions, DCs exposed to VEGF-A during both the differentiation phase (with rhGM-CSF and rhIL-4) and the subsequent TNF-α-induced maturation phase exhibited significantly reduced CD80 and CD83 expression compared with untreated controls (MFI=1) (p=0.009 and p=0.006, respectively) (Fig. 2B), indicating a marked impairment in their maturation. VEGFR-1 blockade with D16F7 mAb significantly restored CD80 expression to control levels (p=0.044 versus VEGF-A alone), while leaving CD83 unaffected (Fig. 2B). At variance, in our experimental setting, HLA-DR expression showed a modest upward trend following VEGF-A exposure (p=0.06), in line with previous reports suggesting that tolerogenic DCs may display a HLA-DR^{high} phenotype despite their suppressive function [9]. VEGFR-1 blockade did not significantly affect HLA-DR expression compared with VEGF-A alone (Fig. 2B). Overall, these findings underscore an

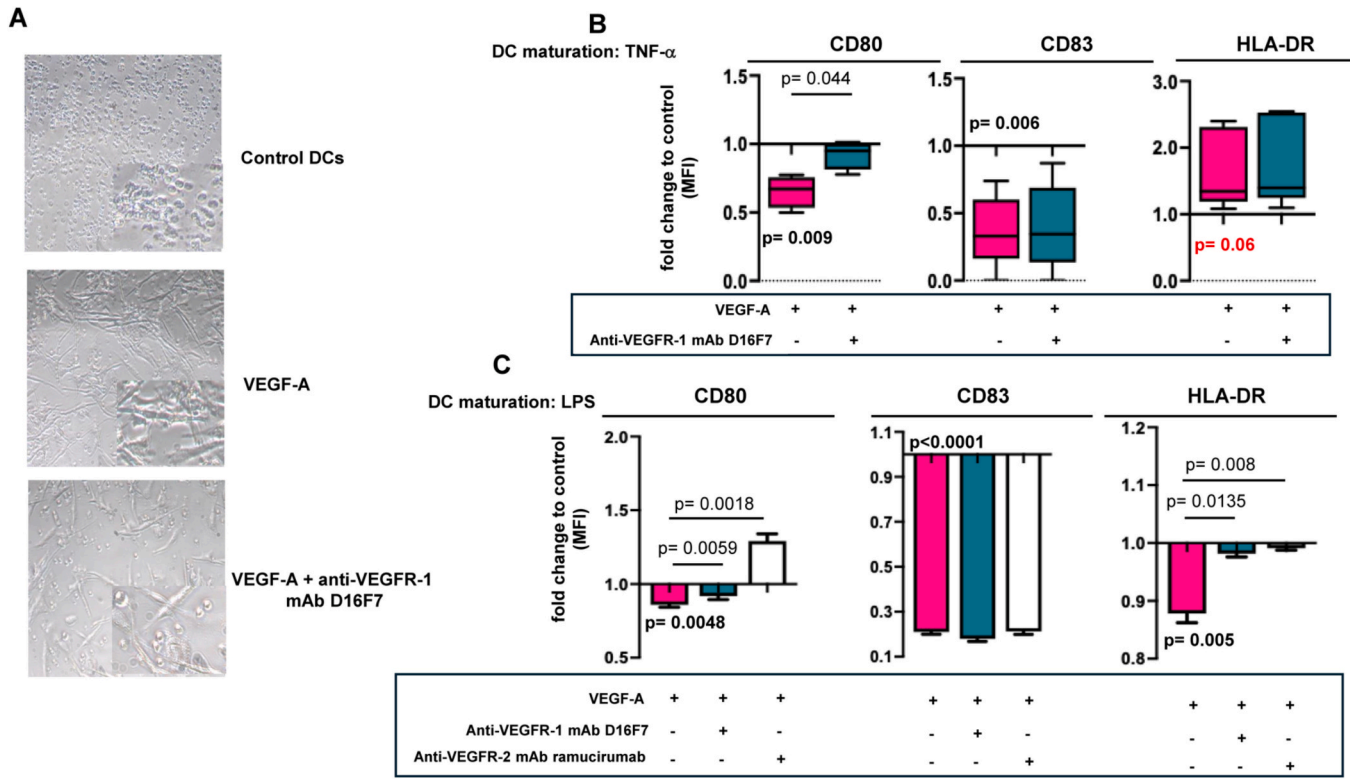

Fig. 2. VEGFR-1 blockade with D16F7 mAb partially restores DC maturation impaired by VEGF-A. PBMC-derived DCs were differentiated with rhGM-CSF + rhIL-4 ± VEGF-A and analysed after TNF-α or LPS-induced maturation. (A) Morphology: control DCs form large, non-adherent clusters with dendritic projections; VEGF-A-conditioned DCs are adherent and spindle-shaped. D16F7 partially reverses this phenotype. (B) TNF-α-induced maturation: VEGF-A decreases CD80 and CD83 expression. D16F7 selectively restores CD80; CD83 and HLA-DR remain unchanged. (C) LPS-induced maturation: VEGF-A downregulates CD80, CD83, and HLA-DR. D16F7 restores CD80 and HLA-DR, whereas VEGFR-2 blockade (ramucirumab, included as control) has a stronger effect on CD80 and comparable effect on HLA-DR. Data are presented as box-and-whisker plots showing the median and interquartile range (B), with whiskers indicating the minimum and maximum values (n = 4–5 independent donors), and bar graphs (C) displaying mean ± SD (n = 3 independent donors). MFI values were normalized as fold changes relative to untreated controls (set to 1). Two-tailed paired t-tests were used for pairwise comparisons, specifically evaluating VEGF-A versus control, and VEGF-A combined with D16F7 or ramucirumab versus VEGF-A alone; $p \leq 0.05$ was considered significant.

important role for VEGFR-1 in the tolerogenic reprogramming of DCs and highlight the potential of VEGFR-1 blockade to mitigate VEGF-A-driven immune dysfunction.

Given previous evidence that VEGF-A suppresses LPS-driven DC maturation more effectively than cytokine-induced DC maturation [49], we examined whether VEGFR-1 blockade with the D16F7 mAb could counteract this suppression. To this end, we assessed CD80, CD83, and HLA-DR expression in DCs exposed to VEGF-A during both the differentiation and the successive LPS-induced maturation phase. Moreover, to delineate receptor-specific contributions, VEGFR-2 inhibition with ramucirumab mAb was included, both as an experimental control and to account for the established role of VEGFR-2 in mediating VEGF-A-induced tolerogenicity of DCs, particularly under LPS-driven maturation conditions [50].

Under these conditions, CD80 expression was consistently downregulated in DCs exposed to VEGF-A during both differentiation and maturation (p=0.0048). Notably, this reduction was reversed by co-treatment with either the anti-VEGFR-1 or, to a greater extent, with the anti-VEGFR-2 mAb (p=0.0059 and p=0.0019, respectively), indicating that both receptors contribute to VEGF-A-mediated impairment of DC co-stimulatory function (Fig. 2C), although to different extents. Similarly, CD83 expression was markedly reduced following VEGF-A exposure (p<0.0001); however, unlike CD80, this reduction was not reversed by blocking either VEGFR-1 or VEGFR-2 (Fig. 2C). In contrast to the effects observed with TNF-α, VEGF-A significantly decreased HLA-DR expression during LPS-induced DC maturation (p=0.005). This effect was effectively counteracted by blockade of VEGFR-1 (p=0.0135) or VEGFR-2 (p=0.008) (Fig. 2C). These different effects likely reflect cross-talks between VEGF-A receptor-mediated pathways and diverse maturation processes engaged by TNF-α and LPS [9].

3.3. *VEGFR-1 blockade by D16F7 mAb reverses PD-1 upregulation in T cells stimulated by VEGF-A-conditioned DCs*

We then assessed whether VEGF-A-conditioned DCs could promote T-cell tolerance by inducing PD-1, as previously reported [51]. DCs were derived from purified $CD14^+$ PBMCs of healthy donors, pulsed with a viral peptide pool, and co-cultured with autologous $CD14^-$ T cells. PD-1 expression was analysed after 14 days, a time point selected to minimise transient, activation-induced PD-1 upregulation and capture sustained expression more closely associated with T-cell exhaustion. T-cell subsets were defined based on PD-1 and CD28 expression to distinguish progressive stages of exhaustion [52]. A trend toward increased frequency of $PD\text{-}1^+CD28^+$ cells was observed in both $CD8^+$ and $CD4^+$ T-cell subsets when co-cultured with viral peptide-loaded DCs conditioned with VEGF-A; this effect was attenuated in the presence of the anti-VEGFR-1 mAb D16F7 (Supplementary Fig. 2). Notably, VEGF-A-conditioned DCs increased PD-1 MFV in co-cultured $PD\text{-}1^+CD8^+$ T cells, particularly in the highly exhausted $PD\text{-}1^+CD28^-$ subset (p=0.03), an effect reversed by VEGFR-1 inhibition (p=0.05) (Fig. 3A,B). A similar pattern was observed in $CD4^+$ T cells, where VEGF-A-conditioned DCs induced a trend toward increased PD-1 expression (p=0.1) in the overall population, which was likewise attenuated by anti-VEGFR-1 treatment (Fig. 3A,C).

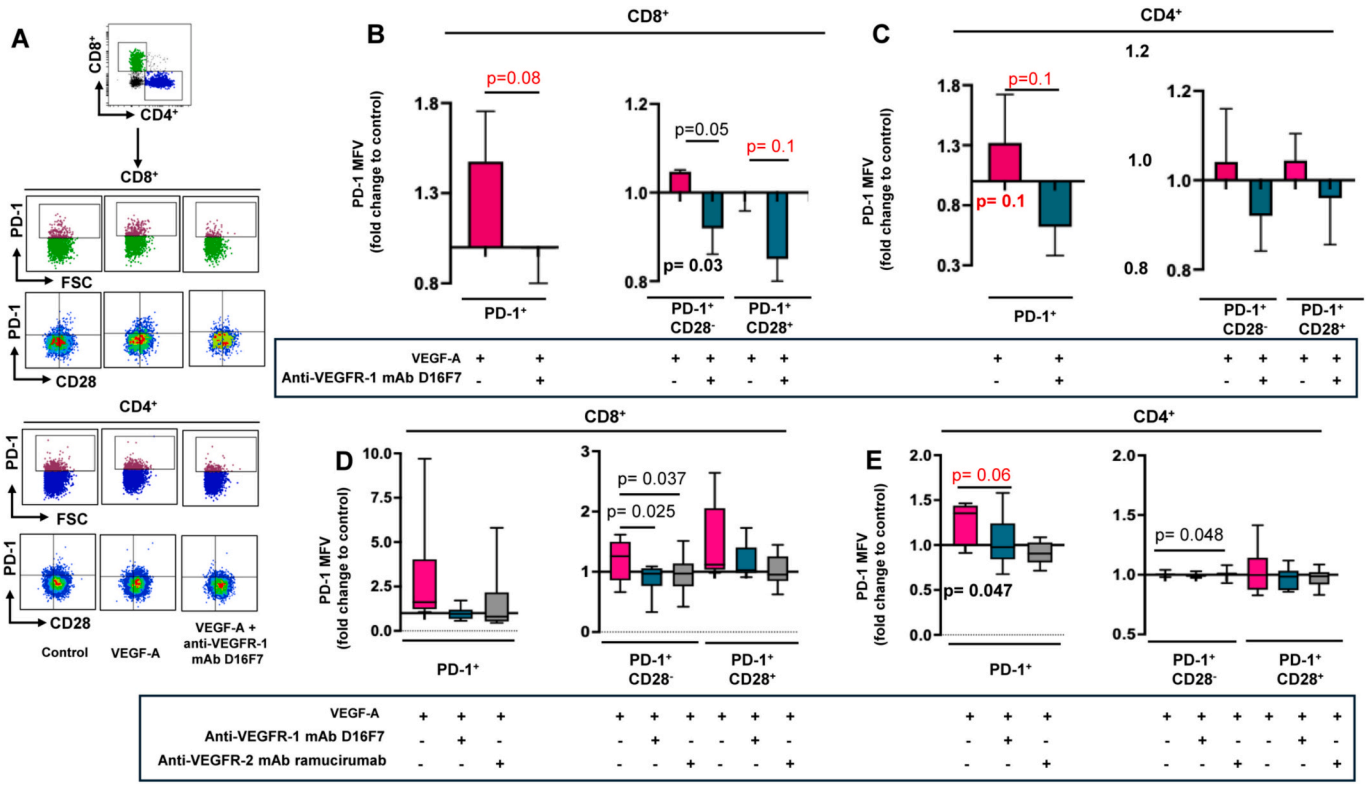

Fig. 3. VEGF-A-conditioned DCs induce PD-1 upregulation in co-cultured T cells, counteracted by the anti-VEGFR-1 mAb D16F7. (A) Gating strategy for $CD8^+$ and $CD4^+$ T-cell subsets based on PD-1/CD28 expression, with representative dot plots. (B,C) Autologous priming: $CD14^+$ monocytes were differentiated into DCs ± VEGF-A/TNF-α, pulsed with viral peptides, and co-cultured with autologous $CD14^-$ T cells for 14 days. PD-1 MFV was assessed in $CD8^+$ (B) and $CD4^+$ (C) $PD\text{-}1^+$ subsets. VEGF-A significantly increases PD-1 MFV in $CD8^+PD\text{-}1^+CD28^-$ T cells; D16F7 reverses this effect. (D,E) Allogeneic mixed lymphocyte reaction: VEGF-A-conditioned DCs maturated with LPS increase PD-1 MFI in $PD\text{-}1^+CD28^-$ T cells, significant in $CD4^+$ cells (D). The anti-VEGFR-1 mAb D16F7 reverses this effect in both lineages; VEGFR-2 blockade (ramucirumab, control) selectively reduces PD-1 in $CD8^+PD\text{-}1^+CD28^-$ T cells (E). Data are shown as mean ± SD from n = 3 (B,C) and 6 (D,E) independent donors. MFI values were normalized as fold changes relative to untreated controls (set to 1). Two-tailed paired t-tests were used for pairwise comparisons, specifically evaluating VEGF-A versus control, and VEGF-A combined with D16F7 or ramucirumab versus VEGF-A alone; $p \leq 0.05$ was considered significant.

These results indicate that VEGFR-1 blockade with D16F7 partially reverses T cell exhaustion, providing proof-of-concept that VEGFR-1 inhibition can modulate immune tolerance.

To further validate these findings, we examined whether VEGF-A-conditioned DCs could promote tolerogenic features in a classical tolerance-inducing mixed lymphocyte reaction (MLR), using $CD14^-$ T cells isolated from unrelated healthy donors. After 14 days of co-culture, VEGF-A exposure increased PD-1 MFV values in $PD\text{-}1^+CD8^+$ T cells. Notably, blockade of either VEGFR-1 (p=0.025) or VEGFR-2 (p=0.037) significantly reduced PD-1 MFV compared with VEGF-A treatment alone within the terminally exhausted $PD\text{-}1^+CD28^-$ subset (Fig. 3D). In $CD4^+$ T cells, VEGF-A-conditioned DCs induced a significant increase in PD-1 expression across the total population (p= 0.047), with a pronounced trend toward reversal observed following VEGFR-1 inhibition with D16F7 mAb (p=0.06) (Fig. 3E). Collectively, these findings indicate that VEGF-A programs DCs toward a tolerogenic phenotype that promotes PD-1 upregulation and T-cell exhaustion, whereas blockade of both, VEGFR-1 and VEGFR-2 partially restores this effect inducing a less exhausted T-cell profile. Although some effects reached only trend-level significance, the consistent observations across both autologous and allogeneic co-cultures underscore VEGFR-1 as a central mediator of VEGF-A-driven, DC-mediated T-cell dysfunction and highlight the potential of VEGFR-1 blockade as a strategy to counteract immune suppression in the TME.

3.4. Blockade of VEGFR-1 with D16F7 preserves T-cell functionality

We next evaluated the direct effects of VEGF-A and selective blockade of VEGFR-1 or VEGFR-2 on the effector function of PBMC-derived $CD8^+$ and $CD4^+$ T cells from healthy donors. To this end, IFN-γ, GrzB, and TNF-α production were measured after a 5-6 h stimulation with plate-bound anti-CD3 mAb and rhIL-2, to capture primary cytokine responses while minimizing confounding effects from secondary activation or proliferation. Analyses were conducted on total T cells and on subsets defined by PD-1 and CD28 expression, which reflect progressive differentiation from naïve/early memory ($PD\text{-}1^-CD28^+$) to terminally exhausted ($PD\text{-}1^+CD28^-$) cells and help identify populations with differential responsiveness to PD-1-targeted immunotherapy [32–34,52]. According to previous reports [23,24,53], VEGF-A modestly yet consistently enhanced IFN-γ production in both total $CD8^+$ T cells (p=0.035) and the $PD\text{-}1^+$ subset (p=0.034) (Fig. 4A,B). This effect was not affected by the anti-VEGFR-1 mAb D16F7 but was significantly reversed by VEGFR-2 blockade (p=0.036 in total $CD8^+$; p=0.025 in $PD\text{-}1^+CD8^+$ T cells), indicating that VEGF-A-induced IFN-γ responses are primarily mediated through VEGFR-2. In contrast, VEGF-A did not significantly alter GrzB expression in either total or $PD\text{-}1^+CD8^+$ T cells, and inhibition of VEGFR-2 did not further modify GrzB levels. Notably, co-treatment with the VEGFR-1-blocking mAb significantly increased GrzB expression in total $CD8^+$ T cells compared with VEGF-A alone (p=0.014) (Fig. 4B), suggesting a potential immunostimulatory effect of VEGFR-1 inhibition in this context. VEGF-A also induced a mild upward trend in TNF-α production in both total (p=0.08) and $PD\text{-}1^+CD8^+$ T cells

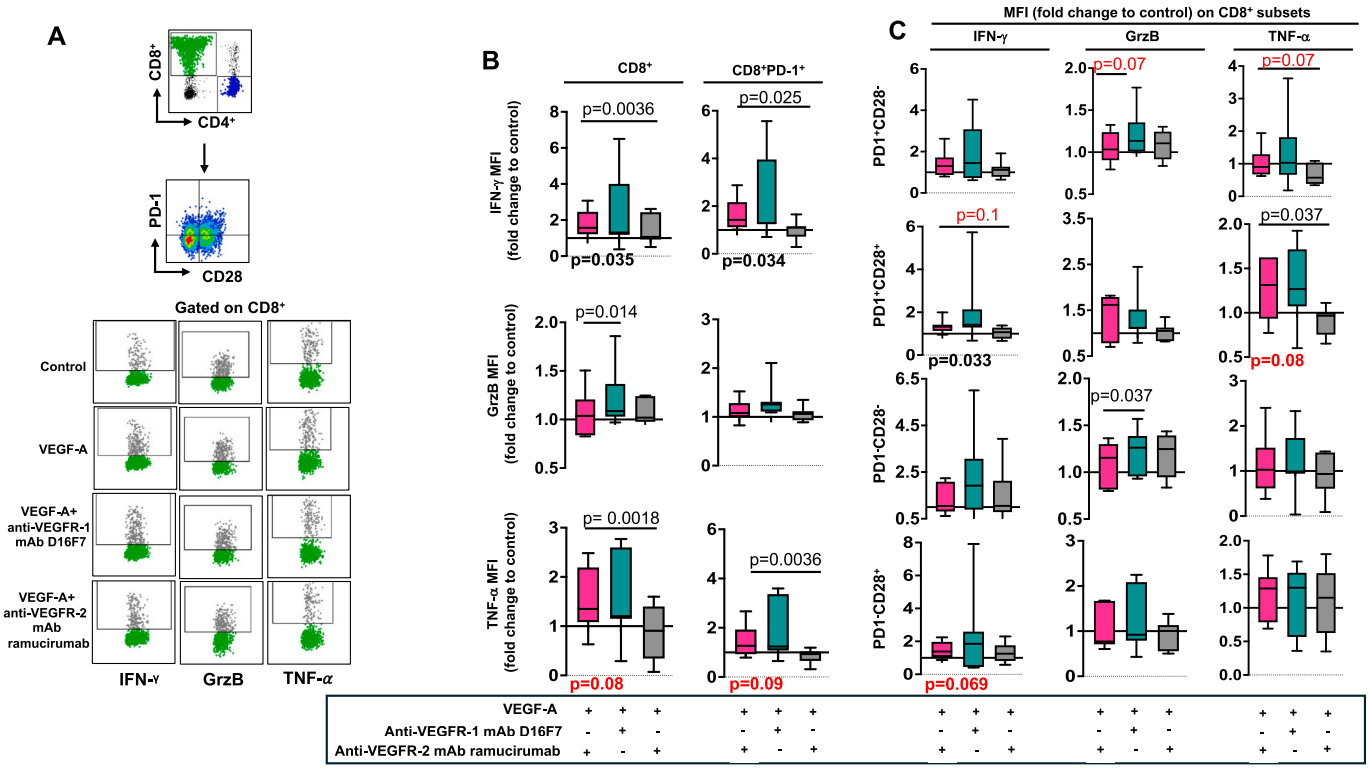

Fig. 4. VEGFR-1 blockade with the D16F7 mAb does not impair short-term VEGF-A-associated cytokine production in CD8$^+$ T cells. PBMCs were stimulated 5–6 h ± VEGF-A with selective VEGFR blockade. (A) Gating strategy for CD8$^+$ and CD4$^+$ T-cell subsets based on PD-1/CD28 expression and representative flow cytometry dot-plots for IFN-γ, GrzB, and TNF-α in total CD8$^+$ cells under indicated culture conditions. (B) VEGF-A increases IFN-γ and induces a trend toward higher TNF-α in total and PD-1$^+$CD8$^+$ T cells, effects reversed by VEGFR-2 blockade but unaffected by D16F7. (C) In PD-1$^+$CD28$^+$ cells, VEGF-A-induced TNF-α is reduced by VEGFR-2 inhibition; VEGFR-1 blockade has no effect. Data are shown as mean ± SD from $n = 7$ independent donors. MFI values were normalized as fold changes relative to untreated controls (set to 1). Two-tailed paired t-tests were used for pairwise comparisons, specifically evaluating VEGF-A versus control, and VEGF-A combined with D16F7 or ramucirumab versus VEGF-A alone; $p \leq 0.05$ was considered significant.

(p=0.09). Notably, this effect was significantly attenuated only by VEGFR-2 blockade in both total CD8$^+$ (p=0.0018) and PD-1$^+$CD8$^+$ T cells (p=0.0036) (Fig. 4A,B), supporting a predominant role for VEGFR-2 in mediating short-term VEGF-A-driven TNF-α upregulation, including within the functionally relevant PD-1$^+$ subset.

Across CD8$^+$ T-cell subsets defined by PD-1 and CD28 expression, VEGF-A modestly increased IFN-γ production in the PD-1$^+$CD28$^+$ population (p=0.033), while showing a trend toward reduction in naïve PD-1$^-$CD28$^+$ cells (p=0.069) (Fig. 4C). Co-treatment with D16F7 did not modify IFN-γ levels in any subset. In contrast, VEGFR-2 inhibition showed a trend toward reduced IFN-γ production specifically in PD-1$^+$CD28$^+$ cells (p=0.1).

VEGF-A did not significantly change GrzB production across CD8$^+$ T-cell subsets. However, VEGFR-1 blockade with D16F7 increased GrzB expression, most notably in PD-1$^-$CD28$^-$ cells (p=0.037), with a strong trend also observed in the highly exhausted PD-1$^+$CD28$^-$ subset (p=0.07) (Fig. 4C), indicating a potential immunostimulatory effect of D16F7 mAb in selected T-cell populations.

Regarding TNF-α, VEGF-A tended to increase its production in PD-1$^+$CD28$^+$ cells (p=0.08), significantly reduced by VEGFR-2 blockade (p=0.037), and showed a trend in PD-1$^+$CD28$^-$ cells (p=0.07). Together, these results indicate that VEGFR-2, rather than VEGFR-1, is the principal mediator of VEGF-A-mediated functional changes in CD8$^+$ T cells. Notably, VEGFR-1 blockade with D16F7 mAb did not reduce effector functions under short-term stimulation; instead, it enhanced GrzB production in selected subsets, supporting its potential benefit as an immunostimulatory strategy.

In total CD4$^+$ T cells and the PD-1$^+$CD4$^+$ subset, VEGF-A significantly increased IFN-γ production (p=0.05 and p=0.038, respectively), consistent with the findings obtained with CD8$^+$ T-cell (Fig. 5A,B). This effect was strongly inhibited by VEGFR-2 blockade (p=0.0034 and p=0.024), indicating that VEGFR-2 is the main mediator of short-term VEGF-A-driven IFN-γ induction in CD4$^+$ T cells. While GrzB expression was largely unaffected by VEGF-A, co-treatment with D16F7 mAb produced only a modest downward trend in total CD4$^+$ T cells (p = 0.06) without impairing the PD-1$^+$ subset. VEGF-A induced a non-significant increase in TNF-α in total CD4$^+$ T cells, which was reduced by both VEGFR-1 (p=0.01) and VEGFR-2 (p=0.05) blockade. In PD-1$^+$CD4$^+$ cells, only VEGFR-2 inhibition significantly decreased TNF-α (p=0.025) (Fig. 5B). Overall, D16F7 mAb had inhibitory effects mainly in total CD4$^+$ T cells, whereas VEGFR-2 blockade consistently suppressed VEGF-A-driven cytokine responses in PD-1$^+$CD4$^+$ cells. Analysis of CD4$^+$ subsets showed that VEGF-A induced a trend toward increased IFN-γ in PD-1$^+$CD28$^+$ cells (p=0.08), which was significantly reduced by VEGFR-2 inhibition (p=0.042) (Fig. 5C). VEGFR-2 blockade also induced a trend towards reduced IFN-γ in PD-1$^+$CD28$^-$ cells (p=0.08). VEGF-A had minimal effects on GrzB across subsets, with uptrend-level significance only in PD-1$^-$CD28$^-$ cells (p=0.06), unaffected by receptor blockade. TNF-α was significantly increased by VEGF-A in PD-1$^+$CD28$^+$ cells (p=0.037) and effectively normalised by VEGFR-2 inhibition (p=0.017) (Fig. 5C).

Overall, VEGF-A-driven short-term cytokine responses in CD4$^+$ T cells are predominantly mediated by VEGFR-2, while VEGFR-1 blockade with D16F7 mAb has a modest impact. VEGFR-2 inhibition effectively suppresses IFN-γ and TNF-α induction, particularly in PD-1$^+$CD28$^+$ cells, highlighting differential receptor-specific roles in modulating CD4$^+$ T-cell effector function.

To assess time-dependent effects of VEGF-A and VEGFR blockade, we extended the stimulation period to 18 hours to evaluate sustained cytokine production and delayed cytolytic programming. To enable an

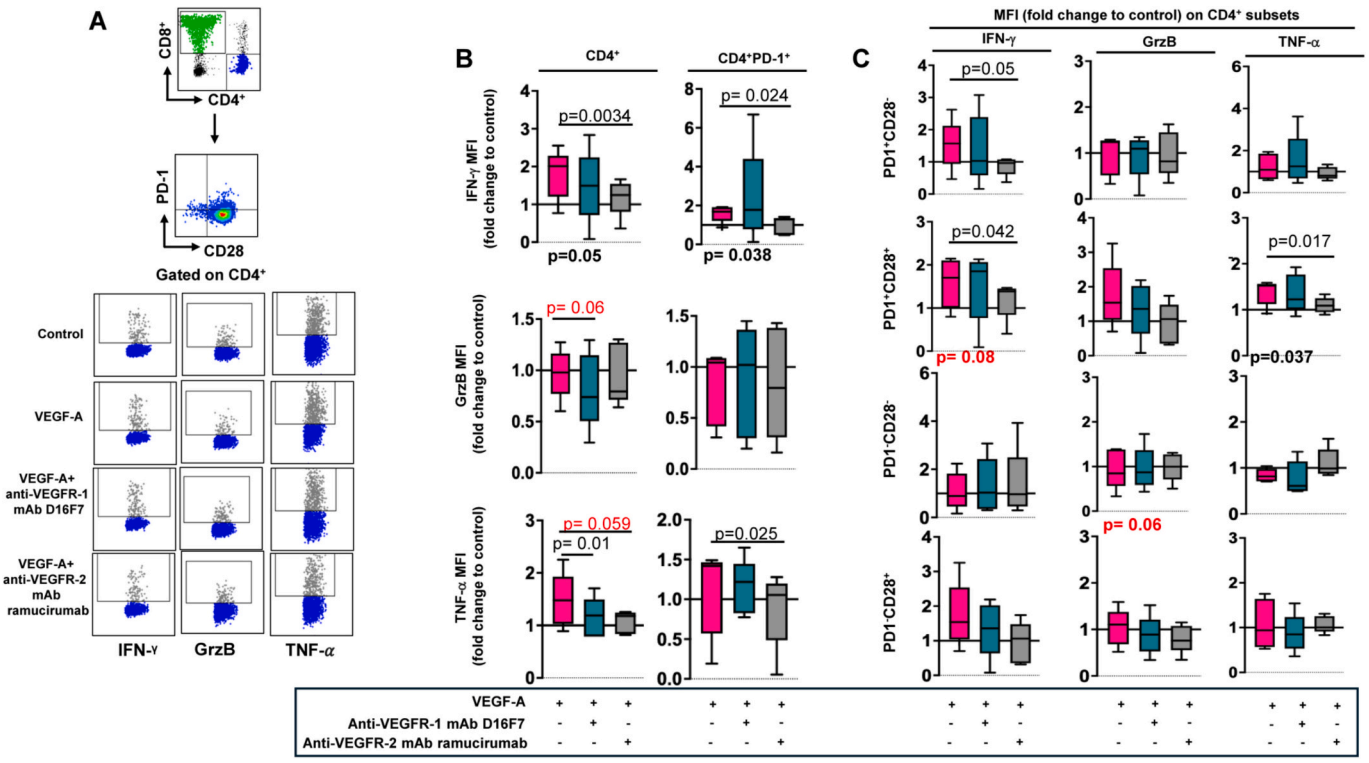

Fig. 5. VEGFR-2 blockade has a stronger effect than D16F7-mediated VEGFR-1 blockade on short-term VEGF-A-induced cytokine production in CD4$^+$ T cells. PBMCs were stimulated 5–6 h ± VEGF-A with selective VEGFR blockade. (A) Gating strategy for CD8$^+$ and CD4$^+$ T-cell subsets based on PD-1/CD28 expression and representative flow cytometry dot-plots for IFN-γ, GrzB, and TNF-α in total CD4$^+$ cells under indicated culture conditions. (B) VEGF-A increases IFN-γ in total and PD-1$^+$ CD4$^+$ T cells, effect reversed by VEGFR-2 blockade, unaffected by D16F7. TNF-α is modestly reduced by D16F7 in total CD4$^+$ T cells; VEGFR-2 inhibition suppresses TNF-α in both total and PD-1$^+$ cells. (C) In PD-1$^+$CD28$^+$ cells, VEGF-A-induced TNF-α is significantly decreased by VEGFR-2 blockade. Data are shown as mean ± SD from $n = 5$ independent donors. MFI values were normalized as fold changes relative to untreated controls (set to 1). Two-tailed paired t-tests were used for pairwise comparisons, specifically evaluating VEGF-A versus control, and VEGF-A combined with D16F7 or ramucirumab versus VEGF-A alone; $p \leq 0.05$ was considered significant.

unbiased assessment of receptor modulation under activation conditions without confounding effects from phenotypic remodelling, analyses were restricted to total and PD-1$^+$ T cells, ensuring reliable assessment of functionally relevant populations.

After 18 h, VEGF-A continued to enhance IFN-γ (p=0.034) and TNF-α (p=0.037) primarily in CD8$^+$ T cells (Supplementary Fig. 3A,B). VEGFR-2 blockade consistently and significantly abolished cytokine production (IFN-γ: total CD8$^+$ p = 0.012, CD8$^+$PD-1$^+$ p=0.002; TNF-α: total CD8$^+$ p= 0.009, CD8$^+$PD-1$^+$ p=0.019). Notably, VEGFR-2 inhibition increased GrzB at 18 h (total CD8$^+$ p = 0.054; CD8$^+$PD-1$^+$ p = 0.035), despite minimal VEGF-A effect on GrzB (Supplementary Fig. 3A,B), suggesting time-dependent regulation of cytolytic programming mediated by VEGFR-2.

In CD4$^+$ T cells, VEGF-A effects were weaker and largely restricted to TNF-α, which was significantly reduced by VEGFR-2 blockade (p=0.017) (Supplementary Fig. 3C). The early mild inhibitory effects of VEGFR-1 blockade were no longer detectable.

Overall, these data indicate that during prolonged stimulation, VEGFR-2 remains the dominant mediator of VEGF-A-driven cytokine responses, while VEGFR-1 has minimal impact.

3.5. *Effect of VEGF-A on the direct induction of Tregs and modulation by D16F7: Impact of PD-1, ICOS and TIM-3*

VEGF-A has been shown to expand Tregs through VEGFR-2, thereby contributing to an immunosuppressive TME [3]. Accordingly, increased Treg frequency correlates with poor prognosis across multiple cancer types [15,16,54]. In addition to VEGFR-2, VEGFR-1 has also been implicated in sustaining the suppressive activity of CD4$^+$ Tregs. Notably, a distinct VEGFR-1^{high} CD4$^+$ Treg subset has been described, suggesting that VEGF-A may broadly influence Treg differentiation and function [19]. Based on these observations, we investigated whether selective VEGFR-1 blockade by D16F7 mAb could counteract VEGF-A-mediated Treg support.

CD4$^+$CD25^{high}CD127^{low} Tregs were isolated from PBMCs of healthy donors and cultured for 7 days with plate-bound anti-CD3 and soluble anti-CD28 Abs plus rhIL-2, in the presence or absence of VEGF-A. PD-1 expression in Tregs has been linked to both suppressive capacity [55] and expansion [56], with PD-1$^+$ICOS$^+$ Tregs representing precursors of highly potent, tissue-resident subsets associated with immune evasion [57,58]. Moreover, TIM-3 marks an activated, effector-like Treg population enriched in tumours, characterised by enhanced suppressor function [59,60]. Accordingly, we assessed the effects of VEGF-A and selective VEGFR-1 or VEGFR-2 blockade on the expression of PD-1, ICOS, and TIM-3, markers of an immunoregulatory phenotype.

After 7 days, VEGF-A significantly upregulated single PD-1 (p=0.0048) and ICOS (p=0.006) (Fig. 6A-C), while appreciably reducing TIM-3 expression (p=0.036) (Fig. 6A,D). Treatment with the VEGFR-1-blocking mAb D16F7 produced a clear trend toward PD-1 downregulation (p=0.08), whereas VEGFR-2 inhibition had no effect on VEGF-A-driven PD-1 induction. Conversely, VEGF-A-induced ICOS upregulation was significantly reduced by VEGFR-2 blockade (p=0.0057) but was not affected by D16F7 mAb (Fig. 6C), suggesting that PD-1 modulation is mainly VEGFR-1-dependent, whereas ICOS induction primarily relies on VEGFR-2. Interestingly, TIM-3 expression was significantly reduced by VEGFR-2 blockade (p=0.05), while reduction mediated by VEGFR-1 inhibition did not reach statistical significance (Fig. 6D).

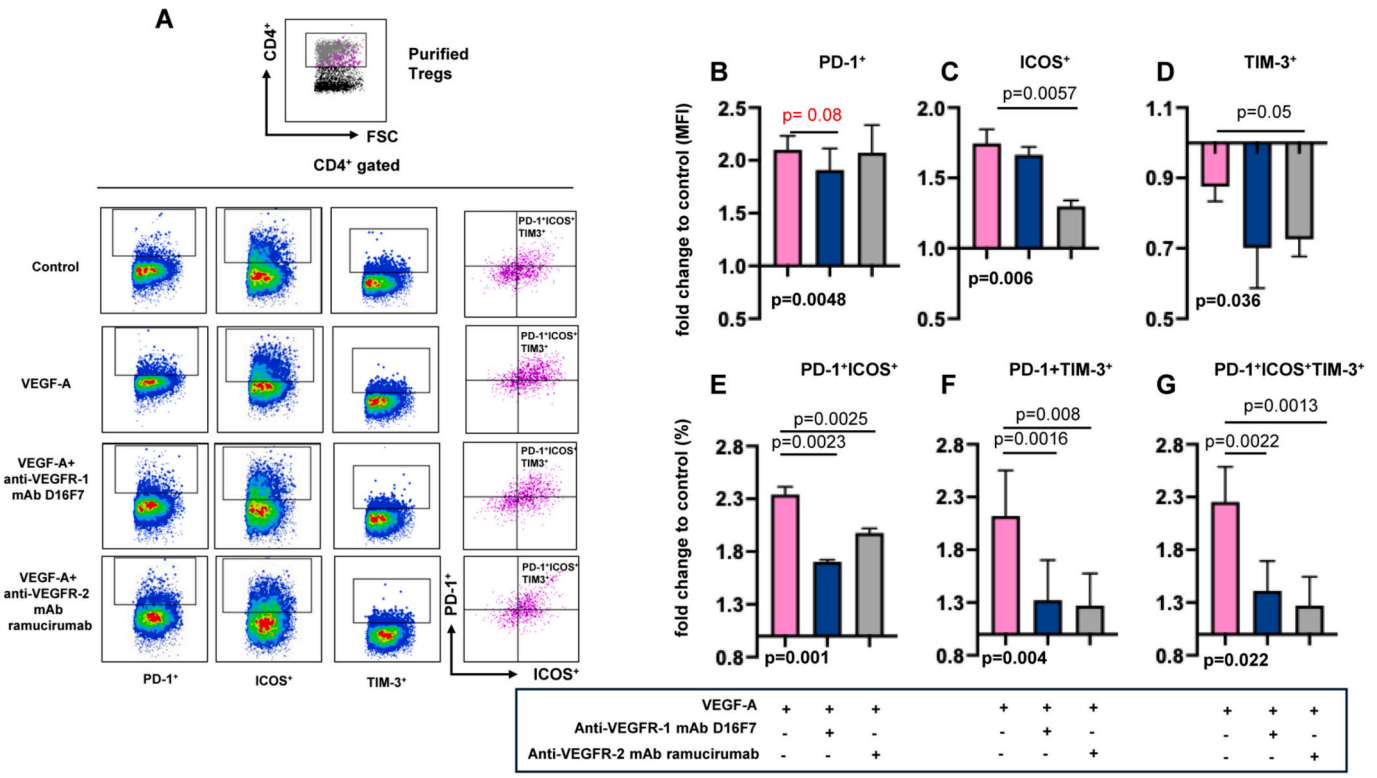

Fig. 6. Blockade of VEGFR-1 and VEGFR-2 reduces the occurrence of an immunosuppressive Treg phenotype through different mechanisms. VEGFR-1 drives PD-1 upregulation, VEGFR-2 mediates ICOS induction. (A) Representative gating for $CD4^+$ Tregs and representative flow cytometry dot-plots for PD-1, ICOS, TIM-3 single positive and PD-1^+ICOS$^+$TIM-3^+ triple positive Tregs under indicated culture conditions. (B) VEGF-A increases PD-1, partially reversed by D16F7; VEGFR-2 blockade has no effect on single ICOS expression. (C) ICOS is upregulated by VEGF-A, reduced by VEGFR-2 blockade, not affected by D16F7. (D) TIM-3 is modestly reduced by VEGF-A, further downregulated by VEGFR-2 blockade. E) VEGF-A increases PD-1^+ICOS$^+$, PD-1^+TIM-3^+, and triple-positive Tregs; effects counteracted by both D16F7 and VEGFR-2 blockade. Data are shown as mean ± SD from n = 3 independent donors. MFI (B,C,D) and percentage (%) (E,F,G) values were normalized as fold changes relative to untreated controls (set to 1). Two-tailed paired t-tests were used for pairwise comparisons, specifically evaluating VEGF-A versus control, and VEGF-A combined with D16F7 or ramucirumab versus VEGF-A alone; $p \leq 0.05$ was considered significant.

Because co-expression of multiple immune checkpoint molecules defines functionally potent Treg subsets, we next examined their combinatorial expression profiles. VEGF-A significantly increased the frequencies of PD-1^+ICOS$^+$ (p=0.001), PD-1^+TIM-3^+ (p=0.004), and PD-1^+ICOS$^+$TIM-3^+ Tregs (p=0.022), expressed as percentage fold changes relative to untreated controls (set to 1) (Fig. 6E-G). Both VEGFR-1 and VEGFR-2 blockade significantly counteracted the VEGF-A-induced expansion of multi-checkpoint Treg subsets, reducing the acquisition of an immunoregulatory phenotype. D16F7 mAb and ramucirumab each decreased the frequencies of PD-1^+ICOS$^+$ Tregs (p=0.0023; p=0.0025), PD-1^+TIM-3^+ Tregs (p=0.0016; p=0.008), and PD-1^+ICOS$^+$TIM-3^+ Tregs (p=0.0022; p=0.0013), respectively (Fig. 6E-G).

Although suppressive function was not directly assessed, the observed phenotypic changes provide a proof-of-concept indication of reduced regulatory potential, consistent with extensive prior literature linking the coordinated expression of these markers to enhanced Treg suppressive activity [3,18,56–61]. Importantly, the concordant modulation of multiple, well-validated inhibitory and activation checkpoints strengthens the biological plausibility of this interpretation. However, dedicated functional assays will be required to assess whether VEGFR-1 blockade directly reduces Treg suppressive capacity.

Overall, these findings demonstrate that VEGF-A enhances the immunosuppressive programming of $CD4^+$ Tregs through coordinately upregulating PD-1, ICOS, and TIM-3, both individually and in combination. Blockade of either VEGFR-1 or VEGFR-2 partially mitigates these effects, indicating that VEGF-A orchestrates Treg activation via complementary receptor pathways. Importantly, the ability of the anti-VEGFR-1 mAb D16F7 to limit VEGF-A-induced PD-1 and multi-checkpoint Treg expansion, without impairing effector T-cell function, underscores its potential to relieve VEGF-A-mediated immune suppression while preserving T-cell-mediated antitumour immunity.

4. Discussion

VEGF-A exerts complex, context-dependent immunoregulatory effects within the TME, promoting DC dysfunction [8,9], T-cell exhaustion [21,22], and Treg expansion [3,18,19], via both VEGFR-1 and VEGFR-2, while inducing transient effector activation under specific conditions [23,24]. Dissecting the distinct contributions of these receptors is therefore essential for identifying the immune subsets most responsive to the modulation of the VEGF-A pathway and for clarifying the nature and magnitude of their functional responses. In this context, the present study was designed as a human PBMC-based proof-of-concept analysis to assess the immunological impact of VEGFR-1 blockade and dissect the contributions of VEGFR-1 versus VEGFR-2 under controlled conditions. Moreover, the use of the anti-VEGFR-1 mAb D16F7, which selectively inhibits membrane-bound VEGFR-1 while preserving soluble VEGFR-1 decoy activity, provides an opportunity to delineate receptor-specific mechanisms underlying VEGF-A-mediated immune regulation [35]. D16F7 has been shown to recognise not only the human VEGFR-1 but also the murine receptor [28] allowing to demonstrate that it exerts antitumor activity in a syngeneic melanoma in vivo model, where it reduces tumour growth and modulates the TME by limiting M2 macrophage, PD-1^+ T cell, and Treg infiltration [35]. Extending these in vivo findings, the present study provides a human immune-cell-focused proof-of-principle analysis, offering insights into DC maturation and tolerogenic programming, VEGFR-1/VEGFR-2 expression, CD28/PD-1-

defined T-cell subset functionality, and suppressive Treg phenotypes. Although obtained in a non-tumour setting, these observations complement prior murine work and underscore the translational potential of VEGFR-1 inhibition as an immunomodulatory strategy. The analysis of VEGFR expression patterns across T-cell subsets indicates that VEGFR-1 is dynamically regulated, with higher expression in PD-1^{+} than in PD-1^{-}CD8^{+} T cells [Fig. 7A] and with notable differences between resting and activated states. VEGFR-2 expression, by contrast, remains comparatively stable. These observations support a model in which VEGFR-1 preferentially operates in T cells already engaged in PD-1-mediated inhibitory programs, whereas VEGFR-2 contributes to impact both early activated and partially exhausted populations. The enrichment of VEGFR-1 in PD-1^{+} T cells aligns with its induction upon antigenic stimulation [27], and prolonged VEGF-A/VEGFR-1 engagement may therefore reinforce inhibitory pathways and metabolic dysfunction associated with exhaustion or regulatory differentiation, as described in VEGF-A-rich tumour settings [22]. However, these findings contribute to inform, although do not establish, the potential relevance of VEGFR-1 blockade in the VEGF-A-enriched TME.

VEGF-A impaired CD80 and CD83 upregulation [Fig. 7B] during TNF-α- and LPS-driven maturation and reduced HLA-DR expression under LPS, thereby promoting a tolerogenic phenotype. Restoration of CD80 expression in both maturation models following VEGFR-1 blockade with D16F7 mAb [Fig. 7B] underscores the critical contribution of VEGFR-1 to VEGF-A-induced DC maturation and tolerogenicity, comparable to the role played by VEGFR-2. Although direct intracellular signalling was not interrogated here, these functional outcomes are consistent with prior studies implicating VEGFR-1-dependent pathways in DC-mediated immune suppression [9,40,41].

The downstream consequences for T-cell priming are consistent with these effects on DCs. VEGF-A-conditioned DCs increased PD-1 expression in responding T cells [Fig. 7B], biasing them toward an exhausted phenotype, whereas inhibition of either VEGFR-1 or VEGFR-2 partially reversed this effect. Together, these findings suggest that disrupting VEGF-A-mediated effects in DCs can limit the transmission of exhaustion-associated cues to T cells during priming. Receptor-specific contributions emerged under short-term T-cell stimulation. Acute VEGF-A exposure enhanced IFN-γ and TNF-α production [Fig. 7C], an effect abrogated almost exclusively by VEGFR-2 blockade, confirming its central role in rapid effector activation. In contrast, VEGFR-1 inhibition preserved these cytokine responses [Fig. 7C]. The minimal impact of D16F7 mAb on CD4^{+} T-cell activation is in agreement with evidence linking VEGFR-1 expression in CD4^{+} T cells to a regulatory phenotype [19]. Our observations partially diverge from those of Gavalas et al., who reported a VEGFR-2-dependent suppression of ovary ascites-derived T-cell proliferation and cytotoxicity after prolonged VEGF-A

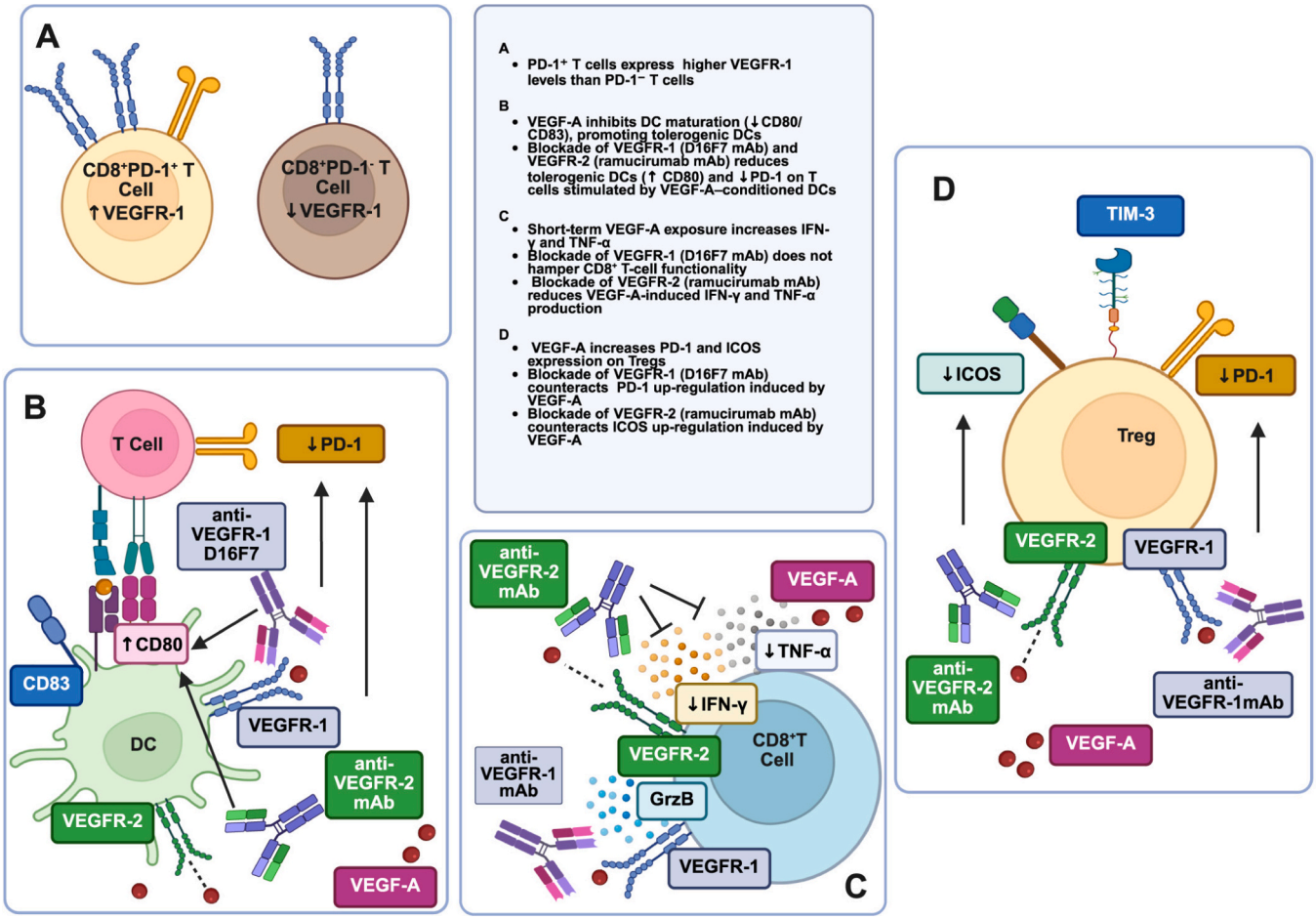

Fig. 7. VEGFR-1 (D16F7) versus VEGFR-2 (ramucirumab) blockade: summary of effects. (A) VEGFR-1 expression in T cells. PD-1^{+} T cells display higher VEGFR-1 expression than PD-1^{-} T cells. (B) VEGF-A-induced tolerogenic DC phenotype. VEGF-A impairs DC maturation (↓CD80/CD83), thereby promoting a tolerogenic DC profile. Blockade of either VEGFR-1 (D16F7 mAb) or VEGFR-2 (ramucirumab mAb) counteracts VEGF-A-induced tolerogenic DC development, as indicated by increased CD80 expression (↑CD80, pointed arrow), and reduced PD-1 levels on T cells stimulated by VEGF-A-conditioned DCs (pointed arrow). (C) T-cell functionality following short-term VEGF-A exposure. VEGF-A enhances IFN-γ and TNF-α production. VEGFR-1 blockade (D16F7 mAb) preserves CD8^{+} T-cell functionality, whereas VEGFR-2 blockade (ramucirumab mAb) reduces VEGF-A-induced IFN-γ and TNF-α production (blunted-end arrows). (D) Regulatory T-cell activation markers. VEGF-A increases PD-1 and ICOS expression on Tregs. VEGFR-1 blockade (D16F7 mAb) counteracts VEGF-A-induced PD-1 up-regulation, while VEGFR-2 blockade (ramucirumab mAb) reduces VEGF-A-induced ICOS up-regulation (pointed arrows). Created with BioRender.

exposure [20]. This divergence likely reflects temporal and contextual differences, as short-term VEGF-A exposure in PBMC-based systems may transiently enhance effector responses through acute metabolic signalling, whereas chronic exposure in tumour-associated fluids promotes sustained inhibitory receptor expression, metabolic exhaustion, and functional decline.

The effects on Tregs revealed an additional layer of VEGF-A-driven immune suppression. VEGF-A induced coordinated upregulation of PD-1 and ICOS, markers associated with highly suppressive and tissue-resident Tregs [57,58]. Consistent with receptor specialisation, VEGFR-1 blockade selectively reduced PD-1 induction, whereas VEGFR-2 inhibition primarily decreased ICOS expression [Fig. 7D]. VEGF-A therefore engages both receptors to activate complementary suppressive pathways. Co-expression of PD-1, ICOS, and TIM-3, characteristic of highly suppressive Tregs [59–61], was diminished by blockade of either receptor, limiting the expansion of these potent regulatory subsets. Although suppressive function was not directly assessed, the observed phenotypic changes provide a proof-of-concept indication of reduced regulatory potential, consistent with extensive prior literature linking the coordinated expression of these markers to enhanced Treg suppressive activity [3,18,56–61]. Importantly, the concordant modulation of multiple, well-validated inhibitory and activation checkpoints strengthens the biological plausibility of this interpretation. However, future work specifically designed to assess Treg function will be required to establish whether VEGFR-1 blockade directly impacts their suppressive capacity.

Taken together, our data indicate that receptor-specific functional segregation is most pronounced at the level of T-cell-intrinsic responses, where VEGFR-1 and VEGFR-2 distinctly regulate short-term effector functionality in defined CD28/PD-1 subsets, whereas VEGF-A-driven DC tolerogenic program reflects a more convergent contribution of both receptors. Notably, Tregs exhibit an intermediate pattern, with receptor-specific modulation of individual checkpoints, PD-1 predominantly regulated by VEGFR-1 and ICOS by VEGFR-2, while the acquisition of multi-checkpoint phenotypes reflects partial convergence at the level of Treg programming.

To our knowledge, this study provides the first integrated, human PBMC-based proof-of-concept study demonstrating that selective blockade of membrane-bound VEGFR-1 with the mAb D16F7 can counteract VEGF-A-induced immune tolerance while preserving VEGFR-2-dependent short-term effector T-cell activation. Importantly, no prior study has directly compared selective VEGFR-1 versus VEGFR-2 blockade on Treg immunosuppressive phenotype and on effector function of T cells characterised by PD-1 and CD28 expression within the same human system.

Although ICIs have transformed cancer therapy, many patients fail to respond or develop resistance, underscoring the need for strategies that overcome VEGF-A-mediated immune suppression [62–65]. While our in vitro conditions cannot model hypoxia, stromal-immune interactions, or chronic VEGF-A exposure in the TME, the preserved VEGF-A-induced cytokine production following VEGFR-1 blockade is particularly relevant given the higher VEGFR-1 expression in $CD8^{+}PD\text{-}1^{+}CD28^{+}$ pre-exhausted T cells, which are most effectively reinvigorated by anti-PD-1 therapies [31–34]. This suggests that VEGFR-1 blockade can relieve inhibitory signals in these cells without compromising effector function and highlights the need for further investigation into how VEGFR-1 blockade modulates distinct T cell subsets within the TME. Accordingly, while this study does not establish therapeutic efficacy, it provides phenotypical and functional insights that can guide the design of future translational studies. These observations highlight the need for further investigation into how VEGFR-1 and VEGFR-2 modulate distinct immune subsets within the TME.

Notably, D16F7 mAb has also been shown to prevent chemotherapy-induced neurotoxicity without compromising antitumor activity [66], suggesting that VEGFR-1 blockade may simultaneously enhance therapeutic efficacy and tolerability.

Overall, our findings underscore the importance of subset-resolved and temporally informed analyses of VEGF-A effects, support VEGFR profiling as a potential biomarker strategy, and position selective VEGFR-1 inhibition as a rational, mechanism-driven approach to alleviate VEGF-A-induced immune dysfunction without impairing T-cell effector capacity.

4.1. Limitations of the Study

Several limitations should be acknowledged. PBMC-based assays and in vitro co-cultures, while informative for dissecting receptor-specific mechanisms, were used as a controlled proof-of-concept system and cannot fully reproduce the spatial organisation, metabolic constraints, hypoxia, stromal-immune interactions, or chronic antigen exposure characteristic of the TME.

The variable donor cohort size (ranging from $n = 3$ to 7, depending on the assay) and inherent inter-individual variability may influence the magnitude of certain effects. While core findings were consistently observed across donors, some observations, particularly those described as trend-level, should be interpreted with appropriate caution due to limited statistical power.

Furthermore, the short-term functional assays employed here (5–6 h and 18 h) were designed to define early receptor-specific immune effects, but do not capture long-term adaptations, likely associated with compensatory signalling or immune remodelling that may arise under sustained VEGF-A exposure in vivo. Extended culture systems will therefore be required to assess the durability of VEGFR-1 blockade effects on T-cell exhaustion, memory formation, and long-term antitumor immunity.

Despite these limitations, the present study, while not establishing therapeutic efficacy, provides a phenotypic and functional rationale to inform the design of future translational studies selectively targeting VEGFR-1 as a strategy to mitigate VEGF-A-driven immune suppression while preserving effector T-cell functionality.

Funding statement

The research leading to these results has received funding from AIRC under IG 2024 - ID. 30361 project – P.I. Graziani Grazia. We also acknowledge financial support under the National Recovery and Resilience Plan (NRRP), Mission 4, Component 2, Investment 1.1, Call for tender No. 104 published on 2.2.2022 by the Italian Ministry of University and Research (MUR), funded by the European Union – NextGenerationEU– Project Title “Preclinical evaluation of the efficacy and cardiac safety of a novel humanized anti-VEGFR-1 monoclonal antibody targeting the tumor and the tumor microenvironment”, CUP E53D23012430006- Grant Assignment Decree No. n 875 adopted on 19/06/2023 by the Italian Ministry of Ministry of University and Research (MUR) (project code MUR 2022EXSWZ2). This work was also supported by the Italian Ministry of Health RC2025 to P.M. Lacal.

CRediT authorship contribution statement

Ornella Franzese: Writing – review & editing, Writing – original draft, Validation, Methodology, Investigation, Formal analysis, Data curation, Conceptualization. **Belinda Palermo:** Methodology, Data curation. **Pedro Miguel Lacal:** Writing – review & editing, Funding acquisition. **Grazia Graziani:** Writing – review & editing, Supervision, Project administration, Funding acquisition, Formal analysis.

Declaration of competing interest

The authors declare that they have no known competing financial interests or personal relationships that could have appeared to influence the work reported in this paper.

Appendix A. Supplementary data

Supplementary data to this article can be found online at https://doi.org/10.1016/j.intimp.2026.116380.

Data availability

Data will be made available on request.

References

[1] C. Lee, M.J. Kim, A. Kumar, H.W. Lee, Y. Yang, Y. Kim, Vascular endothelial growth factor signalling in health and disease: from molecular mechanisms to therapeutic perspectives, Signal Transduct. Target. Ther. 10 (2025) 170, https://doi.org/10.1038/s41392-025-02249-0.

[2] E. Stuttfeld, K. Ballmer-Hofer, Structure and function of VEGF receptors, IUBMB Life 61 (2009) 915–922, https://doi.org/10.1002/iub.234.

[3] M. Bourhis, J. Palle, I. Galy-Fauroux, M. Terme, Direct and indirect modulation of T cells by VEGF-A counteracted by anti-angiogenic treatment, Front. Immunol. 12 (2021) 616837, https://doi.org/10.3389/fimmu.2021.616837.

[4] H. Huang, E. Langenkamp, M. Georganaki, A. Loskog, P.F. Fuchs, L.C. Dieterich, J. Kreuger, A. Dimberg, VEGF suppresses T-lymphocyte infiltration in the tumour microenvironment through inhibition of NF-κB-induced endothelial activation, FASEB J. 29 (2015) 227–238, https://doi.org/10.1096/fj.14-250985.

[5] M. De Palma, D. Biziato, T.V. Petrova, Microenvironmental regulation of tumour angiogenesis, Nat. Rev. Cancer 17 (2017) 457–474, https://doi.org/10.1038/nrc.2017.51.

[6] Y. Huang, B.Y.S. Kim, C.K.F. Chan, S.M. Hahn, I.L. Weissman, W. Jiang, Improving immune–vascular crosstalk for cancer immunotherapy, Nat. Rev. Immunol. 18 (2018) 195–203, https://doi.org/10.1038/nri.2017.145.

[7] N. Horikawa, K. Abiko, N. Matsumura, J. Hamanishi, T. Baba, K. Yamaguchi, Y. Yoshioka, M. Koshiyama, I. Konishi, Expression of vascular endothelial growth factor in ovarian cancer inhibits tumour immunity through the accumulation of myeloid-derived suppressor cells, Clin. Cancer Res. 23 (2017) 587–599, https://doi.org/10.1158/1078-0432.CCR-16-0387.

[8] S. Laxmanan, S.W. Robertson, E. Wang, J.S. Lau, D.M. Briscoe, D. Mukhopadhyay, Vascular endothelial growth factor impairs the functional ability of dendritic cells through id pathways, Biochem. Biophys. Res. Commun. 334 (2005) 193–198, https://doi.org/10.1016/j.bbrc.2005.06.065.

[9] J. Yang, J. Yan, B. Liu, Targeting VEGF/VEGFR to modulate antitumour immunity, Front. Immunol. 9 (2018) 978, https://doi.org/10.3389/fimmu.2018.00978.

[10] R.A. Maldonado, U.H. von Andrian, How tolerogenic dendritic cells induce regulatory T cells, Adv. Immunol. 108 (2010) 111–165, https://doi.org/10.1016/B978-0-12-380995-7.00004-5.

[11] V.K. Raker, M.P. Domogalla, K. Steinbrink, Tolerogenic dendritic cells for regulatory T cell induction in man, Front. Immunol. 6 (2015) 569, https://doi.org/10.3389/fimmu.2015.00569.

[12] V. Kumar, D.I. Gabrilovich, Hypoxia-inducible factors in regulation of immune responses in tumour microenvironment, Immunology 143 (2014) 512–519, https://doi.org/10.1111/imm.12380.

[13] O. Franzese, A. Mascali, A. Capria, V. Castagnola, L. Paganizza, N. Di Daniele, Regulatory T cells in the immunodiagnosis and outcome of kidney allograft rejection, Clin. Dev. Immunol. 2013 (2013) 852395, https://doi.org/10.1155/2013/85239.

[14] C. Lee, M.J. Kim, A. Kumar, H.W. Lee, Y. Yang, Y. Kim, Vascular endothelial growth factor signalling in health and disease: from molecular mechanisms to therapeutic perspectives, Signal Transduct. Target. Ther. 10 (2025) 170, https://doi.org/10.1038/s41392-025-02249-0.

[15] J. Wada, H. Suzuki, R. Fuchino, A. Yamasaki, S. Nagai, K. Yanai, K. Koga, M. Nakamura, M. Tanaka, T. Morisaki, M. Katano, The contribution of vascular endothelial growth factor to the induction of regulatory T-cells in malignant effusions, Anticancer Res. 29 (2009) 881–888.

[16] M. Terme, S. Pernot, E. Marcheteau, F. Sandoval, N. Benhamouda, O. Colussi, O. Dubreuil, A.F. Carpentier, E. Tartour, J. Taieb, VEGFA-VEGFR pathway blockade inhibits tumour-induced regulatory T-cell proliferation in colorectal cancer, Cancer Res. 73 (2013) 539–549, https://doi.org/10.1158/0008-5472.CAN-12-2325.

[17] A. Lapeyre-Prost, M. Terme, S. Pernot, A.L. Pointet, T. Voron, E. Tartour, J. Taieb, Immunomodulatory activity of VEGF in cancer, Int. Rev. Cell Mol. Biol. 330 (2017) 295–342, https://doi.org/10.1016/bs.ircmb.2016.09.007.

[18] Y. Tada, Y. Togashi, D. Kotani, T. Kuwata, E. Sato, A. Kawazoe, T. Doi, H. Wada, H. Nishikawa, K. Shitara, Targeting VEGFR-2 with ramucirumab strongly impacts effector/activated regulatory T cells and CD8+ T cells in the tumour microenvironment, J. Immunother. Cancer 6 (2018) 106, https://doi.org/10.1186/s40425-018-0403-1.

[19] J J.Y. Shin, I.H. Yoon, J.H. Lim, J.S. Shin, H.Y. Nam, Y.H. Kim, W.W. Lee, H.S. Cho, S.H. Hong, J.S. Kim, W.W. Lee, C.G. Park, CD4+VEGFR1high T cell as a novel Treg subset regulates inflammatory bowel disease in lymphopenic mice, Cell. Mol. Immunol. 12 (2015) 592–603, doi:https://doi.org/10.1038/cmi.2015.71.

[20] N.G. Gavalas, M. Tsiatas, O. Tsitsilonis, E. Politi, K. Ioannou, A.C. Ziogas, A. Rodolakis, G. Vlahos, N. Thomakos, D. Haidopoulos, E. Terpos, A. Antsaklis, M. A. Dimopoulos, A. Bamias, VEGF directly suppresses activation of T cells from ascites secondary to ovarian cancer via VEGF receptor type 2, Br. J. Cancer 107 (2012) 1869–1875, https://doi.org/10.1038/bjc.2012.468.

[21] C.G. Kim, M. Jang, Y. Kim, G. Leem, K.H. Kim, H. Lee, T.S. Kim, S.J. Choi, H. D. Kim, J.W. Han, M. Kwon, J.H. Kim, A.J. Lee, S.K. Nam, S.J. Bae, S.B. Lee, S. J. Shin, S.H. Park, J.B. Ahn, I. Jung, K.Y. Lee, S.H. Park, H. Kim, B.S. Min, E.C. Shin, VEGF-A drives TOX-dependent T cell exhaustion in anti-PD-1-resistant microsatellite stable colorectal cancers, Sci. Immunol. 4 (2019) eaay0555, https://doi.org/10.1126/sciimmunol.aay0555.

[22] T. Voron, O. Colussi, E. Marcheteau, S. Pernot, M. Nizard, A.L. Pointet, et al., VEGF-A modulates expression of inhibitory checkpoints on CD8+ T cells in tumours, J. Exp. Med. 212 (2015) 139–148, https://doi.org/10.1084/jem.20140559.

[23] A. Basu, A. Hoerning, D. Datta, M. Edelbauer, M.P. Stack, K. Calzadilla, S. Pal, D. M. Briscoe, Cutting edge: vascular endothelial growth factor-mediated signalling in human CD45RO+ CD4+ T cells promotes Akt and ERK activation and costimulates IFN-γ production, J. Immunol. 184 (2010) 545–549, https://doi.org/10.4049/jimmunol.0902737.

[24] Z. Chen, M. Zhang, Z. Chen, L. Wang, W. Wang, J. Wang, M. He, B. Shi, Y. Wang, VEGF-A enhances the cytotoxic function of CD4+ cytotoxic T cells via the VEGF-receptor 1/VEGF-receptor 2/AKT/mTOR pathway, J. Transl. Med. 21 (2023) 74, https://doi.org/10.1186/s12967-023-03926-w.

[25] Z. Zhang, K.G. Neiva, M.W. Lingen, L.M. Ellis, J.E. Nör, VEGF-dependent tumour angiogenesis requires inverse and reciprocal regulation of VEGFR-1 and VEGFR-2, Cell Death Differ. 17 (2010) 499–512, https://doi.org/10.1038/cdd.2009.152.

[26] P.M. Lacal, G. Graziani, Therapeutic implication of vascular endothelial growth factor receptor-1 (VEGFR-1) targeting in cancer cells and tumour microenvironment by competitive and non-competitive inhibitors, Pharmacol. Res. 136 (2018) 97–107, https://doi.org/10.1016/j.phrs.2018.08.008.

[27] O. Leplina, E. Smetanenko, M. Tikhonova, E. Batorov, T. Tyrinova, N. Pasman, A. Ostanin, E. Chernykh, Binding of the placental growth factor to VEGF receptor type 1 modulates human T cell functions, J. Leukoc. Biol. 108 (2020) 1013–1024, https://doi.org/10.1002/JLB.2A0420-723RR.

[28] G. Graziani, F. Ruffini, L. Tentori, M. Scimeca, A.S. Dorio, M.G. Atzori, C.M. Failla, V. Morea, E. Bonanno, S. D'Atri, P.M. Lacal, Antitumour activity of a novel anti-vascular endothelial growth factor receptor-1 monoclonal antibody that does not interfere with ligand binding, Oncotarget 7 (2016) 72868–72885, https://doi.org/10.18632/oncotarget.

[29] M.G. Atzori, L. Tentori, F. Ruffini, C. Ceci, E. Bonanno, M. Scimeca, P.M. Lacal, G. Graziani, The anti-vascular endothelial growth factor receptor-1 monoclonal antibody D16F7 inhibits glioma growth and angiogenesis in vivo, J. Pharmacol. Exp. Ther. 364 (2018) 77–86, https://doi.org/10.1124/jpet.117.244434.

[30] M.G. Atzori, L. Tentori, F. Ruffini, C. Ceci, L. Lisi, E. Bonanno, M. Scimeca, E. Eskilsson, T. Daubon, H. Miletic, L. Ricci Vitiani, R. Pallini, P. Navarra, R. S. Bjerkvig, S. D'Atri, P.M. Lacal, G. Graziani, The anti-vascular endothelial growth factor receptor-1 monoclonal antibody D16F7 inhibits invasiveness of human glioblastoma and glioblastoma stem cells, J. Exp. Clin. Cancer Res. 36 (2017) 106, https://doi.org/10.1186/s13046-017-0577-2.

[31] E. Hui, J. Cheung, J. Zhu, X. Su, M.J. Taylor, H.A. Wallweber, D.K. Sasmal, J. Huang, J.M. Kim, I. Mellman, R.D. Vale, T cell costimulatory receptor CD28 is a primary target for PD-1-mediated inhibition, Science 355 (2017) 1428–1433, https://doi.org/10.1126/science.aaf1292.

[32] B. Palermo, O. Franzese, G. Frisullo, L. D'Ambrosio, M. Panetta, G. Campo, D. D'Andrea, I. Sperduti, F. De Nicola, F. Goeman, F. Gallina, P. Visca, F. Facciolo, P. Nisticò, CD28/PD1 co-expression: dual impact on CD8+ T cells in peripheral blood and tumour tissue, and its significance in NSCLC patients' survival and ICB response, J. Exp. Clin. Cancer Res. 42 (2023) 287, https://doi.org/10.1186/s13046-023-02846-3.

[33] O. Franzese, B. Palermo, G. Frisullo, M. Panetta, G. Campo, D. D'Andrea, I. Sperduti, R. Taje, P. Visca, P. Nisticò, ADA/CD26 axis increases intra-tumourtumour PD-1^{+}CD28^{+}CD8^{+} T-cell fitness and affects NSCLC prognosis and response to ICB, Oncoimmunology 13 (2024) 2371051, https://doi.org/10.1080/2162402X.2024.2371051.

[34] A.O. Kamphorst, A. Wieland, T. Nasti, S. Yang, R. Zhang, D.L. Barber, B. T. Konieczny, C.Z. Daugherty, L. Koenig, K. Yu, G.L. Sica, A.H. Sharpe, G. J. Freeman, B.R. Blazar, L.A. Turka, T.K. Owonikoko, R.N. Pillai, S.S. Ramalingam, K. Araki, R. Ahmed, Rescue of exhausted CD8 T cells by PD-1-targeted therapies is CD28-dependent, Science 355 (2017) 1423–1427, https://doi.org/10.1126/science.aaf0683.

[35] P.M. Lacal, M.G. Atzori, F. Ruffini, M. Scimeca, E. Bonanno, R. Cicconi, M. Mattei, R. Bernardini, S. D'Atri, L. Tentori, G. Graziani, Targeting the vascular endothelial growth factor receptor-1 by the monoclonal antibody D16F7 to increase the activity of immune checkpoint inhibitors against cutaneous melanoma, Pharmacol. Res. 159 (2020) 104957, https://doi.org/10.1016/j.phrs.2020.104957.

[36] M.E. Keir, M.J. Butte, G.J. Freeman, A.H. Sharpe, PD-1 and its ligands in tolerance and immunity, Annu. Rev. Immunol. 26 (2008) 677–704, https://doi.org/10.1146/annurev.immunol.26.021607.090331.

[37] M. Piao, N. Zhang, J. Li, C. Li, Z. Xun, L. Zhang, S. Wang, B. Sun, S. Li, X. Yang, X. Yang, H. Wang, H. Zhao, Peripheral blood PD-1^{+} T lymphocytes as biomarkers in liquid biopsies for solid tumours: clinical significance and prognostic applications, Int. Immunopharmacol. 147 (2025) 114052, https://doi.org/10.1016/j.intimp.2025.114052.

[38] J.H. Esensten, Y.A. Helou, G. Chopra, A. Weiss, J.A. Bluestone, CD28 costimulation: from mechanism to therapy, Immunity 44 (2016) 973–988, https://doi.org/10.1016/j.immuni.2016.04.020.

[39] T. Wu, J.H.L. Tan, W.X. Sin, Y.H. Luah, S.Y. Tan, M. Goh, M.E. Birnbaum, Q. Chen, L.F. Cheow, Cell granularity reflects immune cell function and enables selection of

lymphocytes with superior attributes for immunotherapy, Adv. Sci. (Weinh.) 10 (2023) e2302175, https://doi.org/10.1002/advs.202302175.
[40] M.M. Dikov, J.E. Ohm, N. Ray, E.E. Tchekneva, J. Burlison, D. Moghanaki, S. Nadaf, D.P. Carbone, Differential roles of vascular endothelial growth factor receptors 1 and 2 in dendritic cell differentiation, J. Immunol. 174 (2005) 215–222, https://doi.org/10.4049/jimmunol.174.1.215.
[41] D.I. Gabrilovich, H.L. Chen, K.R. Girgis, H.T. Cunningham, G.M. Meny, S. Nadaf, D. Kavanaugh, D.P. Carbone, Production of vascular endothelial growth factor by human tumours inhibits the functional maturation of dendritic cells, Nat. Med. 2 (1996) 1096–1103, https://doi.org/10.1038/nm1096-1096.
[42] N.J. Maney, G. Reynolds, A. Krippner-Heidenreich, C.M.U. Hilkens, Dendritic cell maturation and survival are differentially regulated by TNFR1 and TNFR2, J. Immunol. 193 (2014) 4914–4923, https://doi.org/10.4049/jimmunol.1302929.
[43] F. Granucci, E. Ferrero, M. Foti, D. Aggujaro, K. Vettoretto, P. Ricciardi-Castagnoli, Early events in dendritic cell maturation induced by LPS, Microbes Infect. 1 (1999) 1079–1084, https://doi.org/10.1016/S1286-4579(99)00209-9.
[44] C. Orabona, U. Grohmann, M.L. Belladonna, F. Fallarino, C. Vacca, R. Bianchi, S. Bozza, C. Volpi, B.L. Salomon, M.C. Fioretti, L. Romani, P. Puccetti, CD28 induces immunostimulatory signals in dendritic cells via CD80 and CD86, Nat. Immunol. 5 (2004) 1134–1142, https://doi.org/10.1038/ni1124.
[45] C.M. Prazma, N. Yazawa, Y. Fujimoto, M. Fujimoto, T.F. Tedder, CD83 expression is a sensitive marker of activation required for B cell and CD4+ T cell longevity in vivo, J. Immunol. 179 (2007) 4550–4562, https://doi.org/10.4049/jimmunol.179.7.4550.
[46] C.M. Prazma, T.F. Tedder, Dendritic cell CD83: a therapeutic target or innocent bystander? Immunol. Lett. 115 (2008) 1–8, https://doi.org/10.1016/j.imlet.2007.10.001.
[47] P. Jin, T.H. Han, J. Ren, S. Saunders, E. Wang, F.M. Marincola, D.F. Stroncek, Molecular signatures of maturing dendritic cells: implications for testing the quality of dendritic cell therapies, J. Transl. Med. 8 (2010) 4, https://doi.org/10.1186/1479-5876-8-4.
[48] J. Lu, J. Zhao, J. Zhao, J. Ma, K. Liu, H. Yang, Y. Huang, Z. Qin, R. Bai, P. Li, W. Yan, M. Zhao, Z. Dong, VEGF-A-induced immature DCs not mature DCs differentiation into endothelial-like cells through ERK1/2-dependent pathway, Cell Biochem. Funct. 29 (2011) 294–302, https://doi.org/10.1002/cbf.1752.
[49] A. Takahashi, K. Kono, F. Ichihara, H. Sugai, H. Fujii, Y. Matsumoto, Vascular endothelial growth factor inhibits maturation of DCs induced by LPS, but not by proinflammatory cytokines, Cancer Immunol. Immunother. 53 (2004) 543–550, https://doi.org/10.1007/s00262-003-0466-8.
[50] K. Mimura, K. Kono, A. Takahashi, Y. Kawaguchi, H. Fujii, Vascular endothelial growth factor inhibits the function of human mature dendritic cells mediated by VEGF receptor-2, Cancer Immunol. Immunother. 56 (2007) 761–770, https://doi.org/10.1007/s00262-006-0234-7.
[51] H.C. Probst, K. McCoy, T. Okazaki, T. Honjo, M. van den Broek, Resting dendritic cells induce peripheral CD8+ T cell tolerance through PD-1 and CTLA-4, Nat. Immunol. 6 (2005) 280–286, https://doi.org/10.1038/ni1165.
[52] B.C. Miller, D.R. Sen, R. Al Abosy, K. Bi, Y.V. Virkud, M.W. LaFleur, K.B. Yates, A. Lako, K. Felt, G.S. Naik, M. Manos, E. Gjini, J.R. Kuchroo, J.J. Ishizuka, J. L. Collier, G.K. Griffin, S. Maleri, D.E. Comstock, S.A. Weiss, F.D. Brown, A. Panda, M.D. Zimmer, R.T. Manguso, F.S. Hodi, S.J. Rodig, A.H. Sharpe, W.N. Haining, Subsets of exhausted CD8 T cells differentially mediate tumour control and respond to checkpoint blockade, Nat. Immunol. 20 (2019) 326–336, https://doi.org/10.1038/s41590-019-0312-6.
[53] F. Mor, F.J. Quintana, I.R. Cohen, Angiogenesis–inflammation cross-talk: vascular endothelial growth factor is secreted by activated T cells and induces Th1 polarization, J. Immunol. 172 (2004) 4618–4623, https://doi.org/10.4049/jimmunol.172.7.4618.
[54] Y. Pan, H. Zhou, Z. Sun, Y. Zhu, Z. Zhang, J. Han, Y. Liu, Q. Wang, Regulatory T cells in solid tumour immunotherapy: effect, mechanism and clinical application, Cell Death Dis. 16 (2025) 277, https://doi.org/10.1038/s41419-025-07544-w.
[55] H.J. Park, J.S. Park, Y.H. Jeong, J. Son, Y.H. Ban, B.H. Lee, L. Chen, J. Chang, D. H. Chung, I. Choi, S.J. Ha, PD-1 upregulated on regulatory T cells during chronic virus infection enhances the suppression of CD8+ T cell immune response via the interaction with PD-L1 expressed on CD8+ T cells, J. Immunol. 194 (12) (2015) 5801–5811, https://doi.org/10.4049/jimmunol.1401936.
[56] D. Cai, G. Wang, X. Zhang, X. Guo, The role of PD-1/PD-L1 axis in Treg development and function: implications for cancer immunotherapy, Onco Targets Ther 12 (2019) 8437–8445, https://doi.org/10.2147/OTT.S221340.
[57] M. Delacher, C.D. Imbusch, A. Hotz-Wagenblatt, J.P. Mallm, K. Bauer, M. Simon, D. Riegel, A.F. Rendeiro, S. Bittner, L. Sanderink, A. Pant, L. Schmidleithner, K. L. Braband, B. Echtenachter, A. Fischer, V. Giunchiglia, P. Hoffmann, M. Edinger, C. Bock, M. Rehli, B. Brors, C. Schmidl, M. Feuerer, Precursors for nonlymphoid-tissue Treg cells reside in secondary lymphoid organs and are programmed by the transcription factor BATF, Immunity 52 (2020) 295–312.e11, https://doi.org/10.1016/j.immuni.2019.12.002.
[58] M.C. McGee, T. Zhang, N. Magazine, R. Islam, M. Carossino, W. Huang, PD-1 and ICOS counter-regulate tissue resident regulatory T cell development and IL-10 production during flu, Front. Immunol. 13 (2022) 984476, https://doi.org/10.3389/fimmu.2022.984476.
[59] A.S. Gautron, M. Dominguez-Villar, M. de Marcken, D.A. Hafler, Enhanced suppressor function of TIM-3^{+} FoxP3^{+} regulatory T cells, Eur. J. Immunol. 44 (2014) 2703–2711, https://doi.org/10.1002/eji.201344392.
[60] Z. Liu, E.L. McMichael, G. Shayan, J. Li, K. Chen, R. Srivastava, L.P. Kane, B. Lu, R. L. Ferris, Novel effector phenotype of Tim-3+ regulatory T cells leads to enhanced suppressive function in head and neck Cancer patients, Clin. Cancer Res. 24 (18) (2018) 4529–4538, https://doi.org/10.1158/1078-0432.CCR-17-1350.
[61] D.Y. Li, X.Z. Xiong, ICOS+ Tregs: a functional subset of Tregs in immune diseases, Front. Immunol. 11 (2020) 2104, https://doi.org/10.3389/fimmu.2020.02104.
[62] O. Franzese, F. Torino, M.P. Fuggetta, A. Aquino, M. Roselli, E. Bonmassar, A. Giuliani, S. D'Atri, Tumour immunotherapy: drug-induced neoantigens (xenogenization) and immune checkpoint inhibitors, Oncotarget 8 (2017) 41641–41669, https://doi.org/10.18632/oncotarget.16335.
[63] O. Franzese, G. Graziani, Role of PARP inhibitors in cancer immunotherapy: potential friends to immune activating molecules and foes to immune checkpoints, Cancers (Basel) 14 (2022) 5633, https://doi.org/10.3390/cancers14225633.
[64] A. Aquino, N. Bianchi, A. Terrazzan, O. Franzese, Protein kinase C at the crossroad of mutations, cancer, targeted therapy and immune response, Biol.-Basel 12 (2023) 1047, https://doi.org/10.3390/biology12081047.
[65] O. Franzese, Tumour microenvironment drives the cross-talk between co-stimulatory and inhibitory molecules in tumour-infiltrating lymphocytes: implications for optimizing immunotherapy outcomes, Int. J. Mol. Sci. 25 (2024) 12848, https://doi.org/10.3390/ijms252312848.
[66] A. Toti, E. Lucarini, V. Ferrara, C. Parisio, C. Ciampi, E. Gerace, L. Micheli, F. Margiotta, D. Venturi, T. Mello, P.M. Lacal, G. Graziani, G. Mannaioni, C. Ghelardini, L. Di Cesare Mannelli, The dual role of VEGF-A in a complex in vitro model of oxaliplatin-induced neurotoxicity: pain-related and neuroprotective effects, Neurotherapeutics 22 (2025) e00532, https://doi.org/10.1016/j.neurot.2025.e00532.